European Journal of Medicinal Chemistry 140 (2017) 155–171

Contents lists available at ScienceDirect

European Journal of Medicinal Chemistry

journal homepage: http://www.elsevier.com/locate/ejmech

Research paper

Design, synthesis and structure-activity relationship studies of a focused library of pyrimidine moiety with anti-proliferative and anti-metastasis activities in triple negative breast cancer

Dahong Yao [a], Yuxin Zhou [c, d], Lingjuan Zhu [a], Liang Ouyang [c], Jin Zhang [c], Yingnan Jiang [a, b], Yuqian Zhao [a], Dejuan Sun [a], Shilin Yang [a, *], Yang Yu [b, **], Jinhui Wang [a]

[a] School of Traditional Chinese Materia Medica, Shenyang Pharmaceutical University, Shenyang 110016, China
[b] Institute of Traditional Chinese Medicine & Natural Products, Jinan University, Guangzhou 510632, China
[c] State Key Laboratory of Biotherapy and Cancer Center, West China Hospital, Sichuan University, Collaborative Innovation Center for Biotherapy, Chengdu 610041, China
[d] College of Science, China Agricultural University, No. 2 Yuanmingyuan West Road, Haidian District, Beijing 100193, China

ARTICLE INFO

Article history:
Received 7 July 2017
Received in revised form
16 August 2017
Accepted 30 August 2017

Keywords:
Triple-negative breast cancer
Cell death
Autophagy
Metastasis

ABSTRACT

Triple-negative breast cancer (TNBC) is a clinical conundrum with distinct clinical and pathologic features, which is characterized by high aggression, poor prognosis, and lack of targeted therapies. In this study, based on the structural features of type II kinase inhibitors, we designed and synthesized a focused library of 41 pyrimidine derivatives possessing potent anti-proliferation activity, Y29 showed the most potent activity against MDA-MB-231 cells. Subsequently, we carried out target prediction, homology modeling, molecular docking, dynamics simulation and determination of enzymatic activity. The results suggested that PDGFR-β was its potential target. In vitro experiments revealed that Y29 attenuated metastasis by PDGFR-β inhibition-induced autophagy and could enhance autophagy-related cell death through AKT-MAPK feedback loop in MDA-MB-231 cells.

1. Introduction

Breast cancer is the most common malignancy in women, and one of the three most common cancers worldwide, along with lung and colon cancer [1]. Early breast cancer has been considered potentially curable with the development of therapeutic methods in the past years [2]. While Triple-negative breast cancer (TNBC), accounting for 10–17% of all breast carcinomas, a heterogeneous and aggressive disease, is still incurable because of its susceptible resistance and high metastatic properties [3]. TNBC is characterized by estrogen receptor (ER) negative, progesterone receptor (PR) negative and Receptor tyrosine-protein kinase erbB-2 (HER2) negative [4]. TNBC has distinct molecular features compared with other types of tumors. For instance, EGFR, c-Kit and p53 are usually overexpressed and TP53 gene mutations are also catholically observed in TNBC [5]. Additionally, p16, cyclin E and E2F3 are elevated in mRNA levels, while the levels of Rb and cyclin D1 are lower [6]. Currently, chemotherapy still plays a central role in the treatment of TNBC. In recent years, accumulating drugs have been exploited for the treatment of TNBC. Small molecules targeting aberrant DNA repair have been developed, such as PARP inhibitors (AZD2281; BSI-201) [7] and DNA transcription inhibitor (Trabectedin) [8]. Antiangiogenesis, Bevacizumab and Sunitinib have been applied to clinical [9]. EGFR targeting inhibitors showed potent antiproliferative activity, such as Cetuximab, Erlotinib [10,11]. Epigenetic modifications (Trichostatin A, Butyrate, Vorinostat) [12], Src inhibitor (Dasatinib) [13] and PI3K/Akt pathway (Everolimus) [14] also showed therapeutic potential. Despite the advanced development of abovementioned anticancer agents, since triple-negative breast cancer is susceptibly resistant to current targeting therapies and its highly metastatic property, clinical goals are mainly prolongation of survival and maintaining quality of life. TNBC is a clinical conundrum with distinct clinical and pathologic features, which is characterized by high aggression, poor prognosis, and lack of targeted therapies. It is considered as an opportunity to develop novel small molecule drugs with high anti-

* Corresponding author.
** Corresponding author.
E-mail addresses: yangshilin@suda.edu.cn (S. Yang), 1018yuyang@163.com (Y. Yu).

http://dx.doi.org/10.1016/j.ejmech.2017.08.067
0223-5234/

proliferative and metastatic activity for TNBC therapy.

Kinases have emerged as one of the most intensive classes of drug targets with approximately 30 various kinase targets being developed to the stage ready for clinical trials [15]. In recent years, a large number of small molecule kinase inhibitors with high anti-proliferation activity have been reported. Structurally, the pyrimidine ring was often used as a common skeleton in various kinase inhibitors (Fig. 1). Kinase inhibitors were generally divided into 4 types, Type I inhibitors, Type II inhibitors, allosteric inhibitors and covalent inhibitors. The type I inhibitors could recognize the active conformation of the kinases. Type I inhibitors typically have a heterocyclic ring system that occupies the purine binding site, which is commonly substituted by two hydrophobic groups that occupy the adjacent hydrophobic regions I and II. The type I inhibitors have poor selectivity and result in drug resistance. The type II kinase inhibitors could recognize the inactive conformation of the kinases. Movement of the activation loop to the DFG-out conformation exposes an additional hydrophobic binding site directly adjacent to the ATP binding site. The type II kinase inhibitors show low resistance and high selectivity, and have emerged as the focus of the development of kinase inhibitors, such as Imatinib, Lapatinib, sorafenib, Nilotinib and infigratinib [16]. The allosteric inhibitors only bind to the allosteric site, outside the ATP-binding site, which exhibit high degree of kinase selectivity. The covalent inhibitors can form an irreversible, covalent bond to the kinase active site, most frequently by reacting with cysteine residue. But the covalent inhibitors have special requirements on the structure of the target protein, which results in a small range of application.

In this study, based on the structural features of type II inhibitors (Fig. 1), we designed and synthesized a series of different pyrimidine derivatives to inhibit the anti-proliferation of triple negative breast cancer cells (Fig. 2). Firstly, the pyrimidine moiety was utilized as a scaffold to initiate the interactions with kinase hinge as adenine did. Then a substituted aromatic ring was introduced to the 2-or 4-position to occupy the hydrophobic pocket I and a

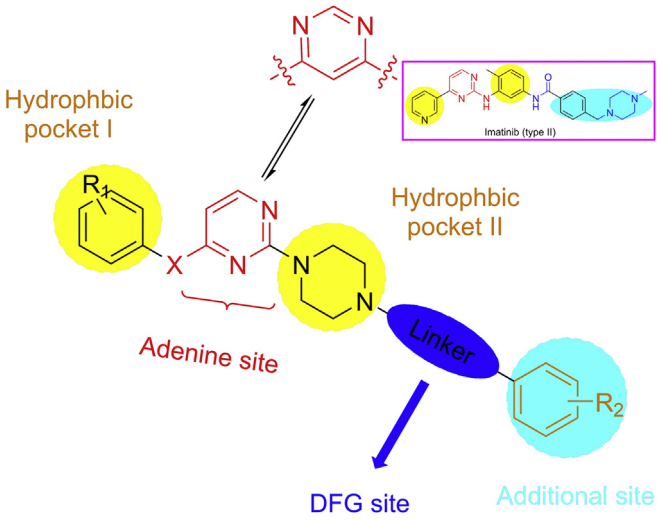

Fig. 2. Design of Type II Kinase inhibitors with pyrimidine moiety.

piperazine group was incorporated into the pyrimidine scaffold to occupy the hydrophobic pocket II. Next, a urea or amide group was used as a linker to interact with the conformation of DFG out, resulting in exposing an additional hydrophobic binding site. Finally, a substituted aromatic ring was induced to occupy the additional hydrophobic binding site. After several rounds of structural optimization based on anti-proliferative activity, a focused library of 41 pyrimidine derivatives was synthesized, which possessed medium to potent anti-proliferation activity, **Y29** showed the most potent activity against MDA-MB-231 cells. Subsequently, we carried out the target prediction, homology modeling, molecular docking, dynamics simulation and determination of enzymatic activity. The results suggested that PDGFR-β was its potential target. The results suggested that PDGFR-β was

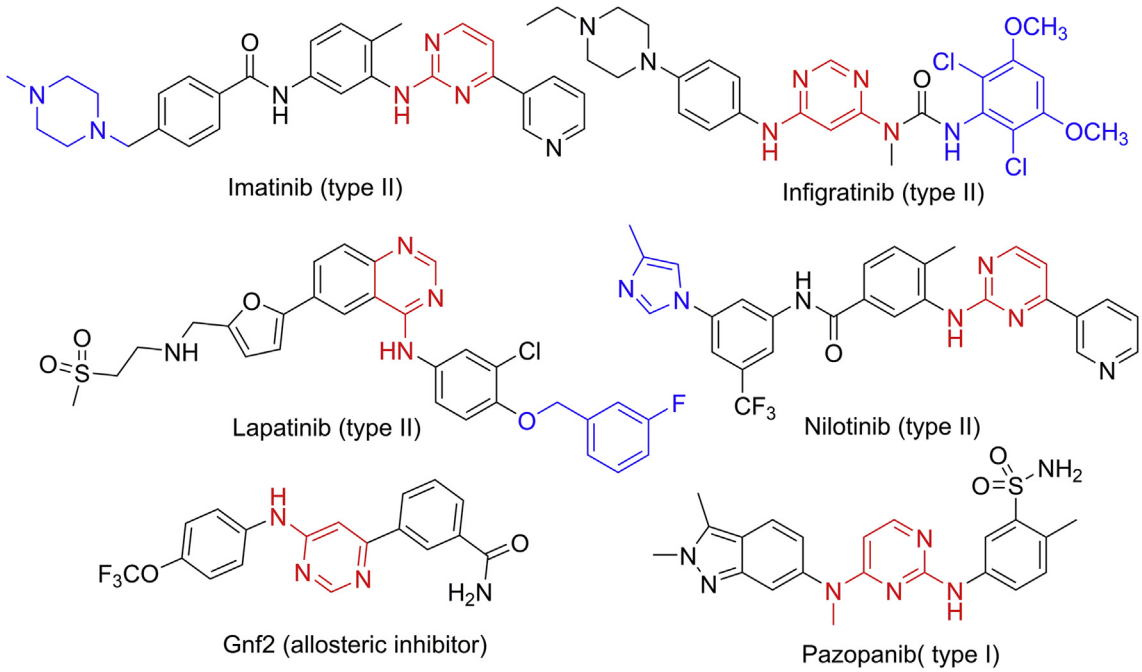

Fig. 1. The structures of several classic anticancer agents with a pyrimidine moiety. The pyrimidine moiety was marked by red, which served as a scaffold binding to the kinase hinge. Compared to type I inhibitors, type II inhibitors have an additional hydrophobic group (marked by blue) that occupy the additional binding site. (For interpretation of the references to colour in this figure legend, the reader is referred to the web version of this article.)

one of its potential targets. In vitro experiments revealed that **Y29** attenuated metastasis by PDGFR-β inhibition-induced autophagy and could enhance autophagy-related cell death through AKT-MAPK feedback loop in MDA-MB-231 cells. Collectively, these findings highlighted a new approach for the development of a novel potential lead for future TNBC therapy.

2. Results and discussion

2.1. Chemistry

The synthesis of compounds **4a-p** was carried out by using commercially available 3, 5-dichlorophenol as the starting materials (Scheme 1). The reaction of 3, 5-dichlorophenol with 2, 4-dichloropyrimdine in acetone yielded intermediate **1**, intermediate **1** reacted with *t*-Butyl 1-piperazincarboxylate to give intermediate **2**. Treatment of intermediate **3** with HCl/MeOH afforded intermediate **3**. The compounds **4a-p** were prepared from intermediate **3** and diverse acyl chlorides. The synthesis of compounds **5a-g** was obtained by sulfonylation of intermediate **3** with appropriate sulfonyl chlorides (Scheme 2). Compounds **6a-g** were synthesized in good yields by the reaction of intermediate **3** and diverse substituted isocyanates in dichloromethane at room temperature (Scheme 3). Treatment of intermediate **3** with bromoacetyl chloride yielded intermediate **7**, and the preparation of compounds **8a-b** was employed by intermediate **7** and 1-methylpiperazine or morpholine in acetonitrile under refluxing for 6 h (Scheme 4). Compounds **12a-c**, **16a-c** and **20a-c** were synthesized by a similar procedure as compounds **5a-g**. The starting materials were replaced with benzylamine or 3-methoxyphenylamine and 4, 6-dichloropyrimdine (Schemes 5–7).

2.2. Evaluation of anti-proliferation activity and SAR in MDA-MB-231 cells

To obtain potent candidate compounds based on the determination anti-proliferation against MDA-MB-231 cells, we designed various aryl substituents on the piperazine to yield compounds **4a-p**. The vitro cytotoxicity-test results revealed that most of these compounds showed weak to moderate cytotoxicity (Table 1). We preferentially induced methyl, chlorine, trifluoromethyl and hydroxyl into meta-position. Compound **4c**, bearing a meta-chlorine, exhibited moderate activity (IC_{50} of 37.8 μM). Replacement of chlorine with trifluoromethyl (**4f**) or hydroxyl (**4i**) resulted in a 1-fold increase of activity. For para-position substituents, trifluoromethyl substituent (**4e**) showed the most potent activity with IC_{50} of 12.5 μM, whereas acetamido substituent (**4h**) lost activity, which suggested that electron-withdrawing group was more favorable than rich electronics group. For the di-substituents, only 2, 4-dichlorophenyl (**4d**) showed a similar activity with **4c**. To further explore SARs, some heterocyclic substituents were incorporated to give **4k-q**. Unfortunately, only two of these compounds exhibited moderate activity with no significant improvement, which indicated that incorporation of these heterocyclic substituents had no contribution to the achievement of activity.

To further explore the chemical space, we also synthesized compounds with a sulfamide as linker (Table 2). Compound **5a**, **5b** and **5f**, with a hydrogen, tertiary butyl and fluorine substituent on para-position respectively, showed no activity. However, *ortho*-methoxyl (**5c**) has a 3-fold increase of activity than *para*-methoxyl (**5d**). Based on the above data, we could draw a conclusion that the linkers, including amide and sulfamide, have no significant distinction for the improvement of activity. Subsequently, the linker was replaced by urea group, leading to compounds **6a-g** (Table 3). Fortunately, most of these compounds presented a significant improvement of activity, owing to the incorporation of urea linker. Compound **6a** bearing a para-position methyl group showed IC_{50} of 11.6 μM. Whereas compound **6d** exhibited a 4-fold decrease of activity, which suggested that the size of the substituent played an important role in activity improvement. On the basis of the above structure analysis, we further explored the various substituents. Ortho-chlorine (**6c**) is more potent than meta-chlorine (**6b**). Next, electron-withdrawing trifluoromethyl was attached into 4- or 3, 5-position to yield **6e** and **6g**. Compound **6e** showed the most potent activity with IC_{50} of 1.54 μM compared with the resulting compounds. We could conclude that the urea linker and electron-withdrawing substituent were very important for anti-proliferation activity.

Subsequently, we synthesized two alkyl substituted derivatives compounds **8a**, **8b**. The results showed a significant decrease of activity (Table 4). On the basis of above SARs, we next explored the replacement of 3, 5-dichlorophenol group with benzylamine and 3-methoxydiphenylamine and combined the urea linker with electron-withdrawing substituents to yield compounds **12a-c**, **16a-c** (Tables 5 and 6). The results revealed that the replacement of bridgehead oxygen with NH had a great activity improvement. Compound **16a** showed the most potent activity with IC_{50} of 1.24 μM. Last, we used 4, 6-dichloropyridine to replace 2, 4-dichloropyridine as the starting material, leading to the new scaffold derivatives **20a-c** (Table 7). The results showed a slight increase of activity (20a vs 16a). Next, we found that compound 20 could inhibit the proliferation of MDA-MB-231 cells in a time- and concentration depended manner, Erlotinib was used as the positive control (Fig. 3). Meanwhile, compound 20 exhibited potent anti-

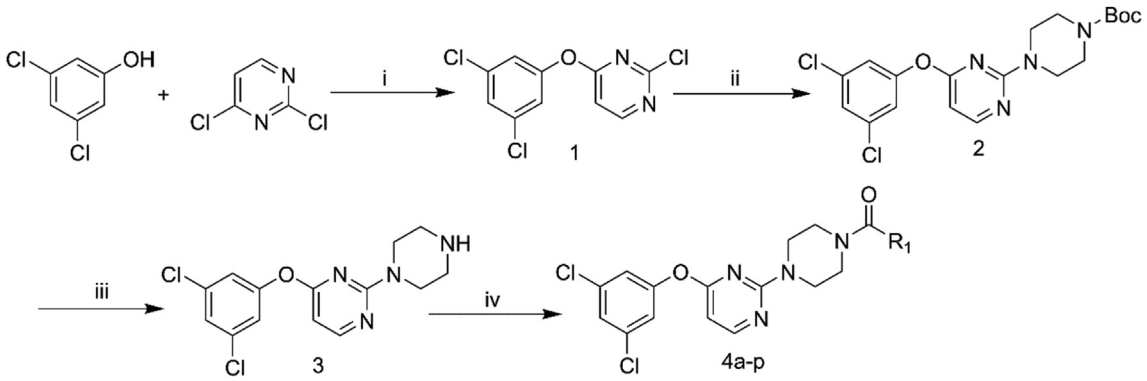

Scheme 1. General synthesis of compounds **4a-p**. Reagents and conditions: (i) acetone, K_2CO_3, r.t., 8 h; (ii) isopropanol, *tert*-butyl 1-piperazinecarboxylate, DIEA, reflux, overnight; (iii) HCl/MeOH, r.t., 6 h; (iv) CH_2Cl_2, R_1COCl, DIEA, r.t.

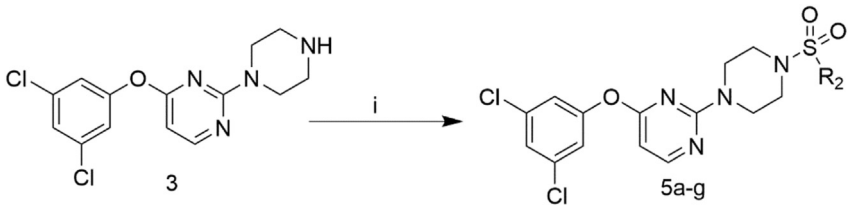

Scheme 2. General synthesis of compounds **5a-g**. Reagents and conditions: (i) CH_2Cl_2, R_2SO_2Cl, DIEA, r.t.

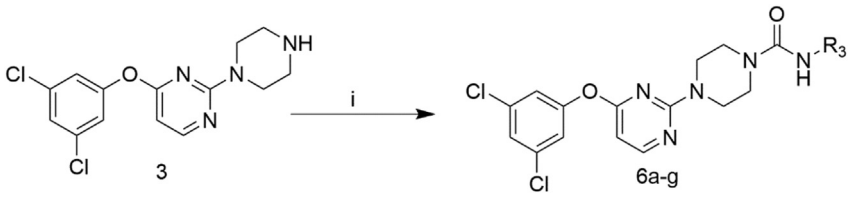

Scheme 3. General synthesis of compounds **6a-g**. Reagents and conditions: (i) CH_2Cl_2, R_3NCO, DIEA, r.t.

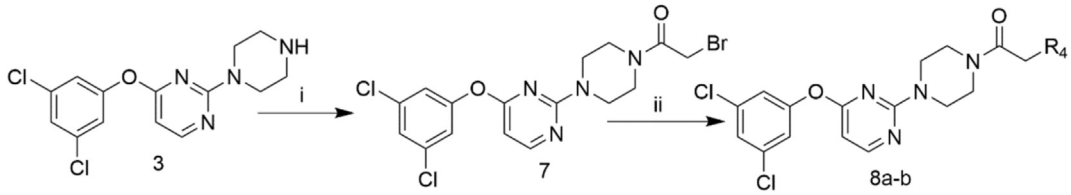

Scheme 4. General synthesis of compounds **8a-b**. Reagents and conditions: (i) CH_2Cl_2, bromoacetyl chloride, DIEA, r.t.; (ii) acetonitrile, DIEA, 1-methylpiperazine or morpholine, reflux, 6 h.

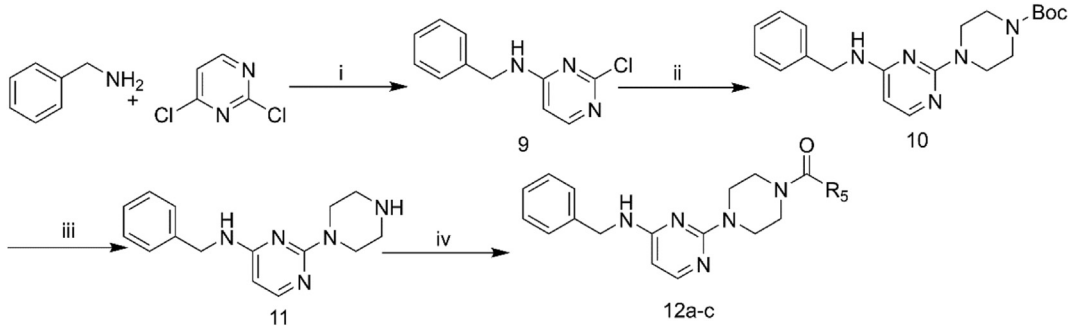

Scheme 5. General synthesis of compounds **12a-c**. Reagents and conditions: (i) ethanol, DIEA, reflux, overnight; (ii) isopropanol, *tert*-butyl 1-piperazinecarboxylate, DIEA, reflux, overnight; (iii) HCl/MeOH, r.t., 6 h; (iv) CH_2Cl_2, R_5COCl, DIEA, r.t.

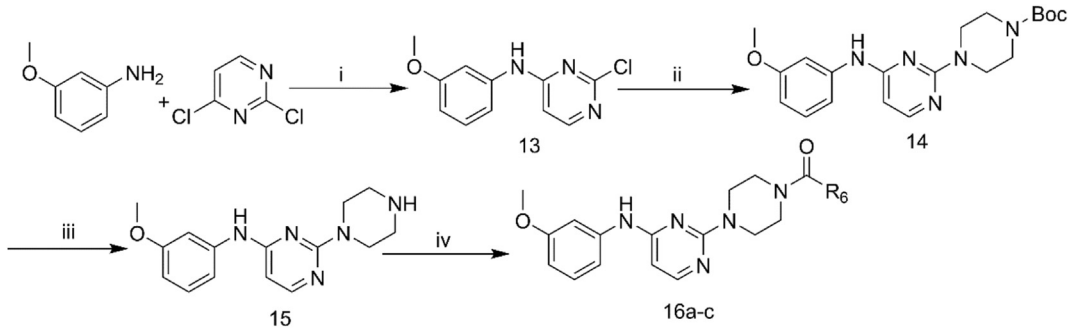

Scheme 6. General synthesis of compounds **16a-c**. Reagents and conditions: (i) ethanol, DIEA, reflux, overnight; (ii) isopropanol, *tert*-butyl 1-piperazinecarboxylate, DIEA, reflux, overnight; (iii) HCl/MeOH, r.t., 6 h; (iv) CH_2Cl_2, R_6COCl, DIEA, r.t.

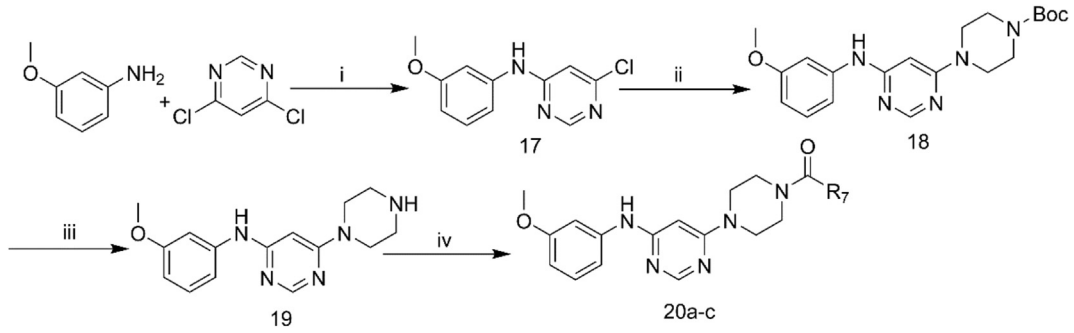

Scheme 7. General synthesis of compounds **20a-c**. Reagents and conditions: (i) isopropanol, H_2SO_4, reflux, 8 h; (ii) isopropanol, *tert*-butyl 1-piperazinecarboxylate, DIEA, reflux, 3 d; (iii) HCl/MeOH, r.t., 6 h; (iv) CH_2Cl_2, R_7COCl, DIEA, r.t.

proliferative activity against other three breast cancer cells (MDA-MB-436, MDA-MB-468 and MCF7) (Fig. S1). So we selected 20a (here after referred as Y29) to further evaluate its *in vitro* anticancer activity and deeper mechanism.

2.3. Prediction potential protein targets and docking and molecular dynamic (MD) stimulation

To determine potential targets of **Y29**, we utilized the Swiss Target Prediction tool [17], a web server for target prediction of bioactive small molecules, to obtain the top 15 potential targets of **Y29** (Table S1). The results presented that these targets were all Tyr kinase class, including receptor tyrosine kinase and non-receptor tyrosine kinase, such as PDGFR and LCK. Given the fact that PDGFR, the most extensively studied member of Tyr kinase family, was considered to be a promising therapeutic target for treatment of breast cancer and combined the "probability value", we assumed that PDGFR-β was the most possible target of **Y29**. Owing to the crystal structure of PDGFR-β has not been resolved, we build the model of PDGFR-B's kinase domain through the Phyre2 web portal Server [18], a web server for protein modeling (Fig. 4A). The parameters were as follows: the template was c2fo0A, confidence is 100% and identity is 39%. Next, a molecular docking was performed by Discovery Studio 3.5 to view the potential interactions. As presented in Fig. 4B and C, **Y29** could form a hydrogen bond with the side chain of Glu87 located in the kinase hinge of ATP binding site. Another key hydrogen bond was reviewed between the trifluoromethyl group of **Y29** and the side chain of His132 in allosteric site, and the phenyl of **Y29** initiated a Pi-Pi interaction with His132. The pyrimidine moiety of **Y29** interacts with Val27 residues to build a Pi-sigma interaction. The above interactions suggested that **Y29** was a potential type II ATP competing inhibitor. Additionally, to further explore the stability of the complex compound **Y29**-PDGFR-β, 10 ns MD simulations were successfully performed on compound Y29- PDGFR-β complexes (Fig. 4D). To gauge whether the MD simulations were stable and whether they were converged, low root-mean-square deviation (RMSD) fluctuations of the systems observed indicates well-behaved systems. To further determine the inhibition of Y29 against PDGFR-β, we conducted the enzymatic activity (IC_{50} = 7.8 μM) (Fig. 4E and F), suggesting that Y29 is a moderate PDGFR-β inhibitor.

2.4. Y29 attenuated metastasis by PDGFR-β inhibition induced autophagy in MDA-MB-231 cells

To gain insight into whether PDGFR-β involved in Y29-mediate cell death, we first evaluated whether Y29 could inhibit MDA-MB-231 cells metastasis. MDA-MB-231 cells harbor Mutant p53 which could drive cancer cells metastasis through PDGFR-β Signaling [19]. We confirmed that Y29 efficiently inhibited MDA-MB-231 cells migration in scratch-wound assays (Fig. 5A). Considering PDGFR-β could directly activate PI3K-AKT signaling [20], we put forward a hypothesis that autophagy and apoptosis involved in Y29-mediate cell death. To assess whether autophagy was a participator in this process, MDA-MB-231 cells were transfected with GFP/mRFP-LC3 plasmid. Obvious aggregation of LC3 puncta was observed after treatment Y29, compared to non-treated cells (Fig. 5B). We also found that Y29 could increase the expression of Beclin1 and LC3II, decrease the expression of p62 (Fig. 5C), indicating that Y29 could induce MDA-MB-231 cells autophagy. To determine whether apoptosis played a role in Y29-induced cell death, we first performed flow cytometry analysis with Annexin-V/PI. The data demonstrated that Y29 could induce MDA-MB-231 cell death but not through classical apoptosis (Fig. 5D), and the expressions of classical apoptosis regulators indicated it as well (Fig. 5E). Next we detected the expressions of PDGFR-β-AKT-regulated autophagy pathways in Y29-treated cells. Firstly, we found that Y29 significantly down-regulated the activity of PDGFR-β by checking its phosphorylation at Tyr740. We also revealed that Y29-treatment induced down-regulation of *p*-AKT (Thr305) and *p*-AKT (ser473), as well as the decrease of the phosphorylation of its downstream member mTOR at ser2448. In addition, we demonstrated that Y29 could induce the up-regulation of *p*-ULK1 (ser317) and *p*-ULK1 (ser555) (Fig. 5F). These results suggested that Y29 attenuated metastasis by PDGFR-β inhibition-induced autophagy in MDA-MB-231 cells. To examine whether Y29 induced autophagy by targeting PDGFR-β, the specific small-interfering RNA was applied for silencing PDGFR-β expression. Interestingly, the silencing of PDGFR-β resulted in a prominent activation of AKT-mTOR-ULK1 autophagy pathway. We found that Y29 displayed almost coordinative effects with PDGFR-β siRNA. When Y29 was used in combination with PDGFR-β siRNA, we did not found any markedly up-regulation of autophagy. These results indicate that Y29 induced autophagy mainly through PDGFR-β (Fig. 5G).

2.5. Y29 could enhance MDA-MB-231 cells autophagy-related cell death through AKT-MAPK feedback loop

Given the complex relationship between PI3K-AKT and MAPK-ERK signaling [21,22], next we determined whether Y29 could affect MAPK-ERK signaling. Firstly, we found that Y29 significantly up-regulated the activity of ERK in nucleus as determined by an increasing fluorescence of anti *p*-ERK (Fig. 6A). Moreover, we revealed that Y29-treatment induced the up-regulation of *p*-ERK (Thr202/Tyr204) in cell lysates (Fig. 6B). In addition, the down-regulation of c-RAF at Ser338 also demonstrated the inhibition of

Table 1
Anti-proliferative activity of compounds **4a-q** in MDA-MB-231 cells.

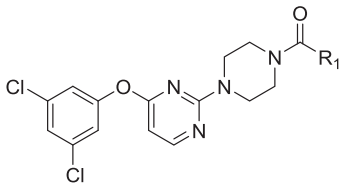

Compound	R_1	Anti-proliferative activity (IC_{50}, μM)[a]
		MDA-MB-231
4a	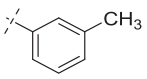	>50
4b		>50
4c	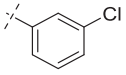	37.79 ± 1.38
4d	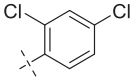	11.82 ± 2.12
4e	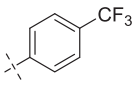	12.50 ± 1.12
4f	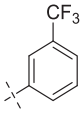	17.9 ± 1.09
4g	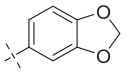	>50
4h	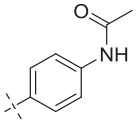	>50
4i	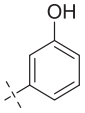	18.4 ± 2.01
4j	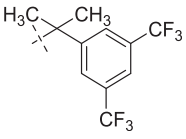	>50
4k	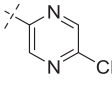	34.8 ± 1.92
4l	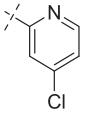	16.7 ± 0.94
4m	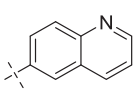	>50

Table 1 (*continued*)

Compound	R_1	Anti-proliferative activity (IC_{50}, μM)[a]
		MDA-MB-231
4n	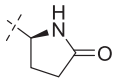	>50
4o	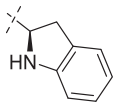	>50
4p		35.2 ± 2.12

[a] Each compound was tested in triplicate; the data are presented as the mean ± SD.

Table 2
Anti-proliferative activity of compounds **5a-g** in MDA-MB-231 cells.

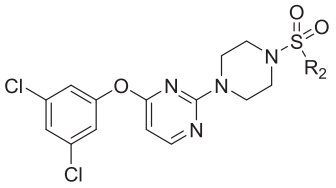

Compound	R_2	Anti-proliferative activity (IC_{50}, μM)[a]
		MDA-MB-231
5a		>50
5b	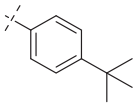	>50
5c	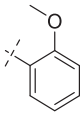	16.79 ± 1.38
5d	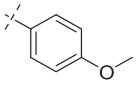	46.82 ± 2.12
5e		24.8 ± 1.18
5f	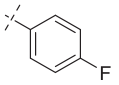	>50
5g	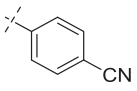	24.8 ± 1.18

[a] Each compound was tested in triplicate; the data are presented as the mean ± SD.

AKT. Interestingly, we found that Y29 didn't affect almost the expression and activity of RAS and MEK (Fig. 6B), indicating the competing and complicated crosstalk between different signaling pathways (Fig. 6C). Together, these findings suggested that Y29

Table 3
Anti-proliferative activity of compounds **6a-g** in MDA-MB-231 cells.

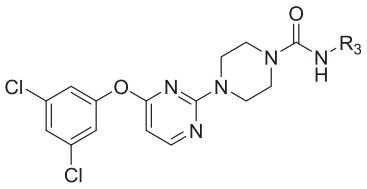

Compound	R_3	Anti-proliferative activity (IC_{50}, μM)[a]
		MDA-MB-231
6a	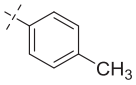	11.6 ± 0.86
6b	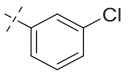	7.9 ± 0.58
6c	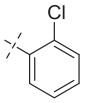	11.0 ± 0.97
6d	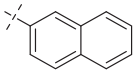	46.82 ± 2.12
6e	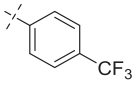	1.54 ± 1.18
6f	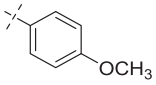	16.4 ± 1.28
6g	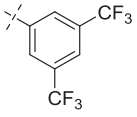	6.74 ± 0.71

[a] Each compound was tested in triplicate; the data are presented as the mean ± SD.

Table 4
Anti-proliferative activity of compounds **8a-b** in MDA-MB-231 cells.

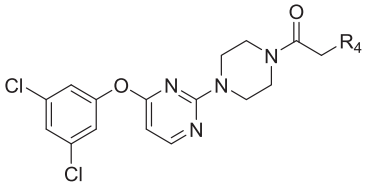

Compound	R_4	Anti-proliferative activity (IC_{50}, μM)[a]
		MDA-MB-231
8a	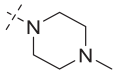	24.7 ± 1.26
8b	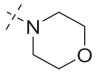	37.6 ± 1.11

[a] Each compound was tested in triplicate; the data are presented as the mean ± SD.

Table 5
Anti-proliferative activity of compounds **12a-c** in MDA-MB-231 cells.

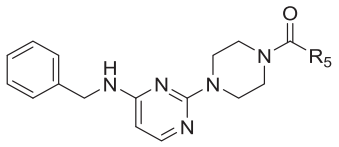

Compound	R_5	Anti-proliferative activity (IC_{50}, μM)[a]
		MDA-MB-231
12a	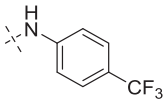	2.45 ± 0.53
12b	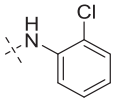	1.59 ± 0.29
12c	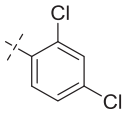	9.79 ± 1.38

[a] Each compound was tested in triplicate; the data are presented as the mean ± SD.

Table 6
Anti-proliferative activity of compounds **16a-c** in MDA-MB-231 cells.

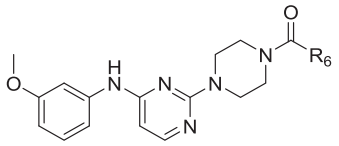

Compound	R_6	Anti-proliferative activity (IC_{50}, μM)[a]
		MDA-MB-231
16a	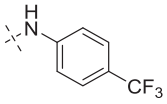	1.24 ± 0.43
16b	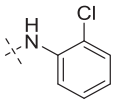	5.26 ± 0.36
16c	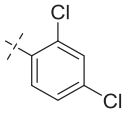	11.32 ± 1.38

[a] Each compound was tested in triplicate; the data are presented as the mean ± SD.

could enhance MDA-MB-231 cells autophagy-related cell death through AKT-MAPK feedback loop.

3. Conclusion

TNBC is a huge threat to women's lives because of his high metastasis and drug resistance, there is no effective targeted therapy. In recent years, the success of kinase inhibitors has led to a major breakthrough in breast cancer treatment. Kinase inhibitors

Table 7
Anti-proliferative activity of compounds **20a-c** in MDA-MB-231 cells.

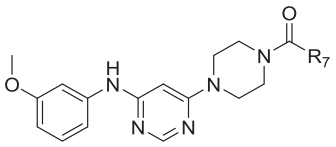

Compound	R_7	Anti-proliferative activity (IC_{50}, μM)[a]
		MDA-MB-231
20a	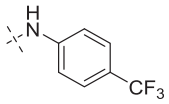	0.73 ± 0.10
20b	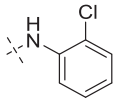	2.8 ± 0.31
20c	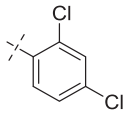	7.23 ± 0.87

[a] Each compound was tested in triplicate; the data are presented as the mean ± SD.

are divided into four types, Type I inhibitors, Type II inhibitors, allosteric inhibitors and covalent inhibitors. The type II kinase inhibitors could recognize the inactive conformation of the kinase, showing lower resistance and higher selectivity than Type I inhibitors. Based on structural characterization of type II kinase inhibitors, we designed and synthesized a focused library of 41 pyrimidine derivatives possessing potent anti-proliferation activity. The results revealed that Y29 showed the most potent anti-proliferation activity. Subsequently, we utilized the Swiss Target Prediction tool to determine potential targets of Y29, the result suggested PDGFR-β was the potential target. To further determine the inhibition of Y29 against PDGFR-β, we conducted the enzymatic activity (IC_{50} = 7.8 μM), suggesting that Y29 is a moderate PDGFR-β inhibitor. Additionally, to gain insight into whether PDGFR-β involved in Y29-mediate cell death, we first evaluated whether Y29 could inhibit MDA-MB-231 cells metastasis. Surprisedly, Y29 efficiently inhibited MDA-MB-231 cells migration in scratch-wound assays. The Western blot assays demonstrated that Y29 attenuated metastasis by PDGFR-β inhibition-induced autophagy in MDA-MB-231 cells. Considering the complex relationship between PI3K-AKT and MAPK-ERK signaling, we evaluated whether Y29 could affect MAPK-ERK signaling. The results confirmed that Y29 could enhance autophagy-related cell death through AKT-MAPK feedback loop in MDA-MB-231 cells. There are some limitations to be addressed in this work. First, although we predicted potential targets for Y29, Y29 just showed a moderate inhibitory activity over PDGFR-β in enzymatic activity. I hold the view that Y29 is more likely to be a multiple kinase inhibitor than a target inhibitor. Y29 showed potent activity *in vitro* and needed to be verified in vivo. Additionally, deeper mechanisms need to be further analyzed. In conclusion, Y29 showed potent anti-proliferative and anti-metastatic activity in MDA-MB-231 cells with novel mechanism. These findings will provide some valuable hints for the development of small molecule drugs for TNBC therapy.

4. Experimental

4.1. Materials and measurements

^{1}H NMR spectra were recorded at 400 MHz. The chemical shifts were recorded in ppm relative totetramethylsilane and with the solvent resonance as the internal standard. Data were reported as follows: chemical shift, multiplicity (s = singlet, d = doublet, t = triplet, q = quartet, m = multiplet), coupling constants (Hz), integration. ^{13}C NMR data were collected at 100 MHz with complete proton decoupling. Chemical shifts were reported in ppm from the tetramethylsilane with the solvent resonance as internal standard. ESI-HRMS spectra were recorded on a commercial apparatus and methanol was used to dissolve the sample. All chemicals were obtained from commercial sources and used without further purification. Column chromatography was carried out on silica gel (300–400 mesh, Qingdao Marine Chemical Ltd, Qingdao, China). Thin layer chromatography (TLC) was performed on TLC silica gel 60 F254 plates. Melting points were uncorrected and determined on Shenguang melting point apparatus (SGW X-4). The purity of compounds was determined to be over 95% (>95%) by reverse-

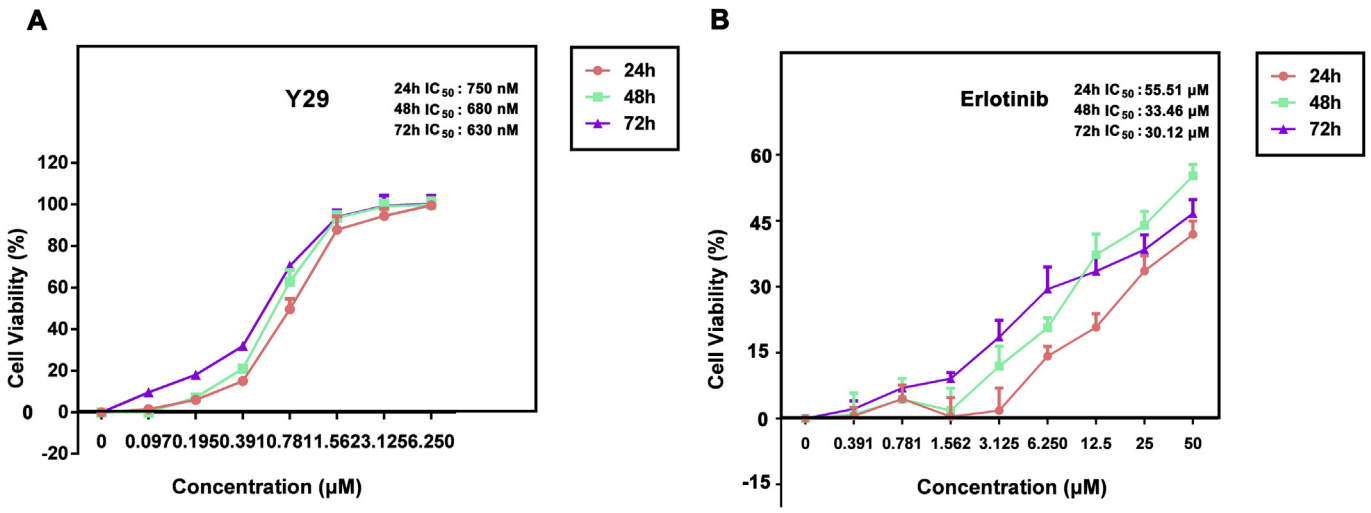

Fig. 3. Y29 inhibited the proliferation of MDA-MB-231 cells. MDA-MB-231 cells were treated with Y29 or Erlotinib with different concentrations, respectively, after treatment 24 h, 48 h and 72 h, MTT assays were performed to measure the proliferation of the cells.

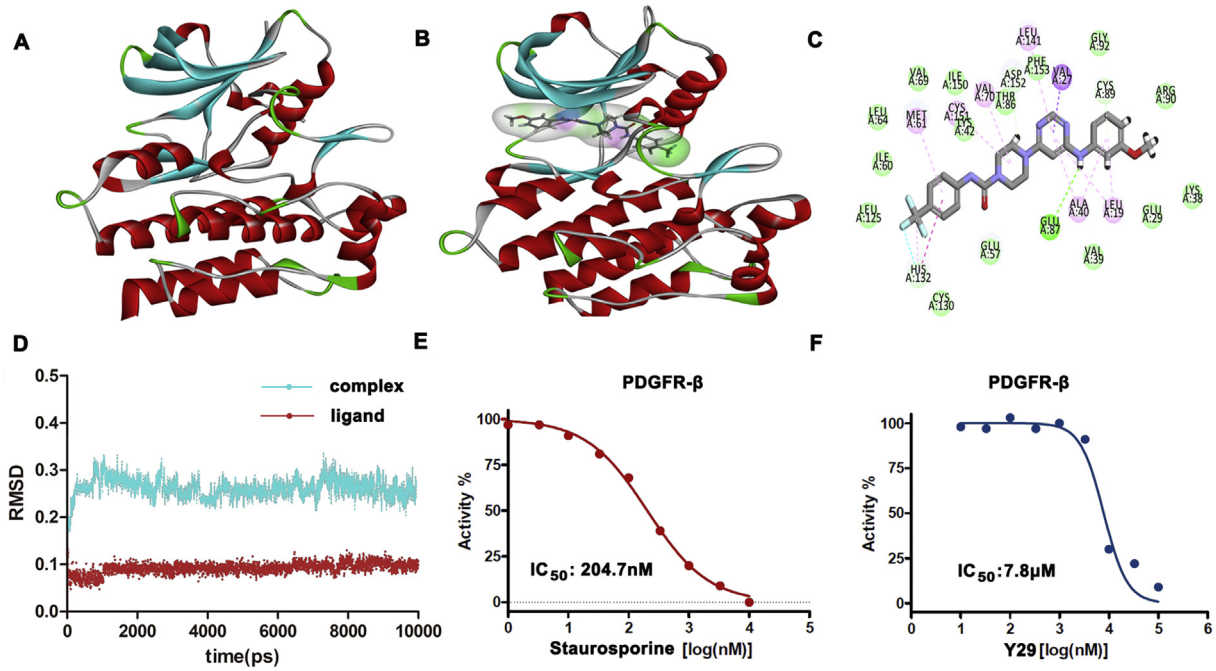

Fig. 4. Molecular modeling, molecule docking, dynamics simulations and enzymatic activity. (A) The homology model of PDGFR-β; (B) Molecule docking of compound Y29 and PDGFR-β. (C) A detailed show of interaction between Y29 and PDGFR-β. (D) Molecular dynamics of compound Y29-PDGFR-β complex. (E) and (F) PDGFR-β kinase assay was performed with Y29 to determine the level of PDGFR-β kinase activity. Staurosporine was used as the reference drug.

phase high performance liquid chromatography (HPLC) analysis. HPLC instrument: SHIMADZU HPLC (Column: Diamonsil C18-WR, 5.0 μM, 4.6 × 250 mm (WondaSil); Detector: SPD-20A Photodiode Array; Injector: SIL-20A Autoinjector; Pump: LC-20AT). Elution: MeOH in water; Flow rate: 1.0 ml/min.

4.2. Synthesis

4.2.1. Synthesis of intermediate **1**

To a solution of 3,5-dichlorophenol (33 mmol) in acetone (100 ml), K_2CO_3 (1.5 eq) was added at room temperature, after 30 min, 2,4-dichloropyrimidine (30 mmol) was added and the resulting mixture was stirred for additional 8 h continually. Upon completion the reaction mixture was filtered and the cake was washed twice by acetone. The combined filtrate was concentrated under reduced pressure to give the crude product. The purity was prepared by re-crystallization from ethyl alcohol, as a white solid, yield 88%. 2-chloro-4-(3,5-dichlorophenoxy)pyrimidine (**1**) ^{1}H NMR (400 MHz, $CDCl_3$), δ(ppm): 8.50 (1H, d, J = 5.5 Hz), 7.31 (1H, m), 7.11 (2H, d, J = 1.8 Hz), 6.88 (1H, d, J = 5.5 Hz); ^{13}C NMR (100 MHz, DMSO-d_6), δ(ppm): 174.6, 167.0, 164.0, 157.9, 139.9, 139.9, 131.5, 126.5, 126.5, 113.2.

4.2.2. Synthesis of intermediate **2**

To a solution of intermediate **1** (10 mmol) in isopropanol (60 ml), DIEA (1.5 eq) and *tert*-butyl 1-piperazinecarboxylate (15 mmol) were added at room temperature. The resulting mixture was allowed to warm up reflux for additional overnight. After completion, the residue was evaporated and added 50 ml water, extracted with dichloromethane (3 × 50 ml). The combined organic layers were washed with saturated aqueous sodium bicarbonate and brine, and then dried over anhydrous sodium sulfate. After removing the solvent under reduced pressure to give the crude oil. The crude oil was purified by silica sel flash chromatography (dichloromethane/methanol 50:1) as a white solid, yield 81%. *Tert*-butyl4-(4-(3,5-dichlorophenoxy)pyrimidin-2-yl)piperazine-1-carboxylate (**2**) ^{1}H NMR (400 MHz, $CDCl_3$), δ(ppm): 8.22 (1H, d, J = 5.6 Hz), 7.24 (1H, m), 7.10 (2H, d, J = 1.7 Hz), 6.12 (1H, d, J = 5.5 Hz), 4.79 (1H m), 3.66 (3H, m), 3.44 (4H, m), 1.47 (9H, s); ^{13}C NMR (100 MHz, DMSO-d_6), δ(ppm): 168.9, 161.4, 160.0, 154.8, 153.4, 135.1, 135.1, 125.5, 125.5, 120.9, 120.9, 96.4, 96.4, 80.0, 80.0, 43.6, 28.4, 28.4, 28.4.

4.2.3. Synthesis of intermediate **3**

A 250 ml round bottom flask was charged with 100 ml methanol saturated by HCl gas at 0 °C, the intermediate **3** (15 mmol) was added in portion under stirring intensely for 6 h. Upon completion, the residue was concentrated and added 50 ml water, the mixture was basified with aqueous NaOH (1 moL/L) till pH = 10 and extracted with ethyl acetate (3 × 50 ml). The combined organic layers were washed with saturated aqueous sodium bicarbonate and brine, and then dried over anhydrous sodium sulfate. After removing the solvent under reduced pressure to give the crude oil. The crude oil was purified by silica sel flash chromatography (dichloromethane/methanol 10:1), as a white solid, yield 92%. 4-(3,5-dichlorophenoxy)-2-(piperazin-1-yl)pyrimidine (**3**) ^{1}H NMR (400 MHz, $CDCl_3$), δ(ppm): 8.21 (1H, d, J = 5.5 Hz), 7.23 (1H, m), 7.11 (2H, d, J = 1.8 Hz), 6.08 (1H, d, J = 5.5 Hz), 3.66 (4H, m), 2.87 (4H, m); ^{13}C NMR (100 MHz, DMSO-d_6), δ(ppm): 173.6, 166.2, 165.6, 158.6, 139.4, 139.4, 130.6, 126.4, 126.4, 100.9, 50.4, 50.4, 49.8, 49.8.

4.2.4. General procedure synthesis of compounds ***4a-p***

Method A. To a solution of intermediate **3** (1 mmol) and DIEA (1.1 mmol) in dichloromethane (10 ml), a solution of R_1COCl (1.1 eq) in dichloromethane (2 ml) was added dropwise at room temperature for 3 h. The mixture was washed with water, saturated aqueous sodium bicarbonate and brine, and then dried over anhydrous sodium sulfate. After removing the solvent under reduced pressure, the crude product was purified by flash chromatography on silica gel, eluting with dichloromethane/methanol

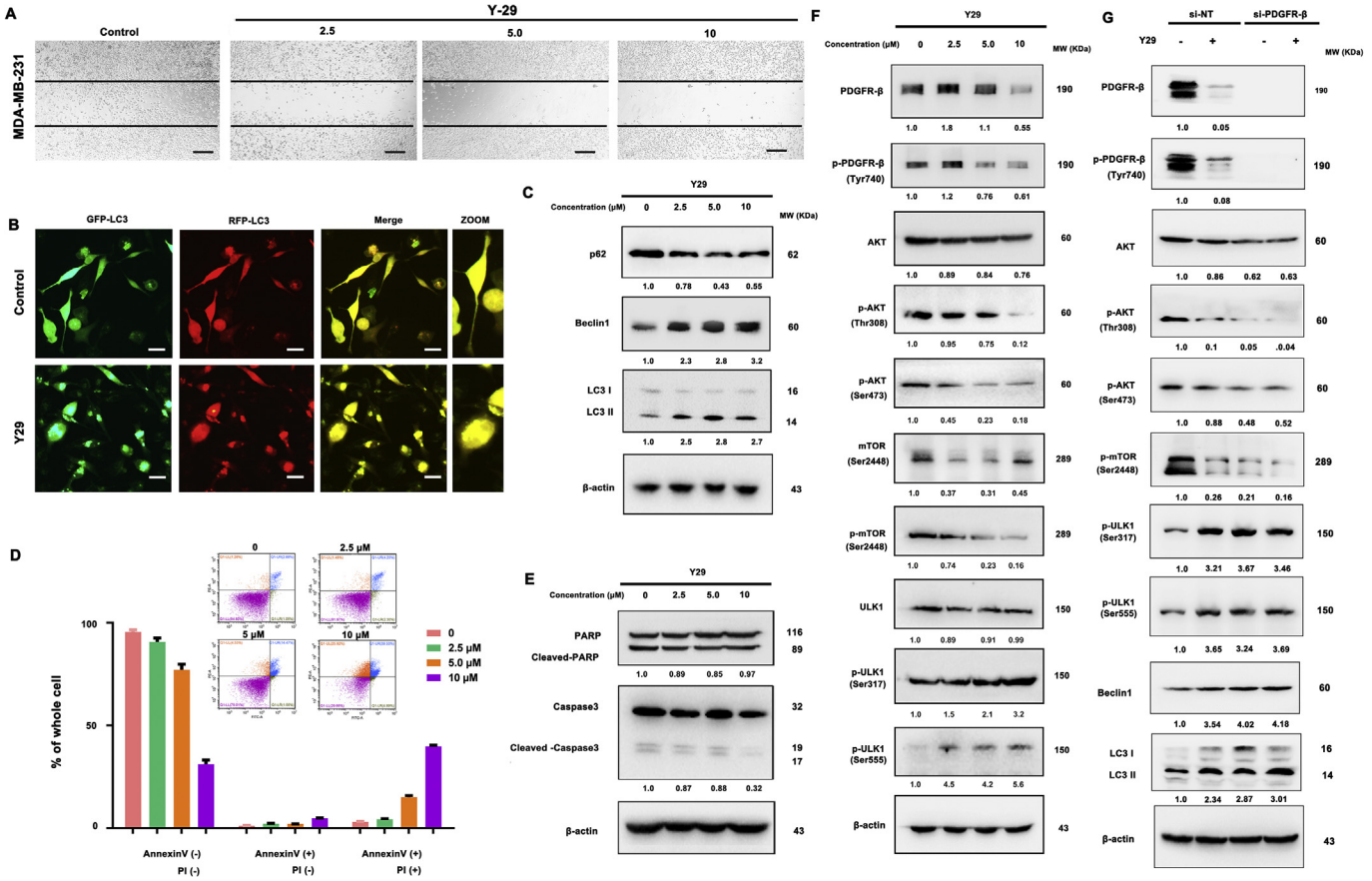

Fig. 5. Y29 attenuated metastasis by PDGFR-β inhibition induced autophagy in MDA-MB-231 cells. (A) MDA-MB-231 cells were treated with Y29 of 2.5, 5.0 and 10 μM, respectively, then scratch wound assays were used to measure the migration capabilities of the cells. Scale bar: 200 μM; (B) MDA-MB-231 cells were transfected with GFP/mRFP-LC3 plasmid, after incubate with 2.5 μM Y29, the GFP-LC3 puncta were observed by fluorescence microscope. Scale bar: 20 μM; (C) MDA-MB-231 cells were treated with different concentrations of Y29 for 24 h and then the expressions of Beclin-1, p62 and LC3 were detected by western blot analysis; (D) MDA-MB-231 cells were treated with different concentrations of Y29 for 24 h, apoptosis ratios were determined by flow cytometry analysis of Annexin-V/PI double staining; (E) MDA-MB-231 cells were treated with different concentrations of Y29 for 24 h and then the expressions of PARP and caspase3 were detected by western blot analysis; (F) The expressions of the PDGFR-β-AKT-ULK1 autophagy signaling were detected by western blot analysis. β-actin was measured as the loading control. (G) MDA-MB-231 cells were transfected with control or PDGFR-β siRNA, followed by treatment with 2.5 μM Y29 for 24 h. Then, the expression levels of PDGFR-β-AKT-ULK1 autophagy signaling were detected by western blot analysis. β-actin was measured as the loading control.

(2–5%), yield 70–95%.

Method B. To a solution of R_1COOH (1 mmol) in DMF (5 ml), DIEA (3 mmol), intermediate **3** (1.1 mmol) and HBTU (1 mmol) were added at room temperature for 10 h. The mixture was diluted with 20 ml water and extracted with ethyl acetate (3 × 20 ml). The combined organic layers were washed with saturated aqueous sodium bicarbonate and brine, and then dried over anhydrous sodium sulfate. After removing the solvent under reduced pressure, the crude product was purified by flash chromatography on silica gel, eluting with dichloromethane/methanol (2–5%), yield 70–95%.

*4.2.4.1. (4-(4-(3,5-dichlorophenoxy)pyrimidin-2-yl)piperazin-1-yl)(m-tolyl)methanone (**4a**).* Prepared by method A, white solid, mp. 164–167 °C, yield 82%. ^{1}H NMR (400 MHz, $CDCl_3$), δ(ppm): 8.23 (1H, d, J = 5.5 Hz), 7.30 (1H, m), 7.23 (3H, m), 7.18 (1H, d, J = 7.4 Hz), 7.09 (2H, d, J = 1.7 Hz), 6.15 (1H, d, J = 5.5 Hz), 3.64 (8H, m), 2.38 (3H, s); ^{13}C NMR (100 MHz, $CDCl_3$), δ(ppm): 170.8, 168.9, 161.3, 160.0, 153.3, 138.6, 135.5, 135.1, 130.6, 128.4, 127.7, 125.6, 124.0, 120.9, 120.9, 96.7, 47.3, 43.8, 43.8, 42.0, 21.4; HRMS (ESI)+ calculated for $C_{22}H_{21}Cl_2N_4O_2$, $[M+H]^+$: m/z 443.1042, found 443.1044; Purity: 99.2% (HPLC).

*4.2.4.2. (4-(4-(2,4-dichlorophenoxy)pyrimidin-2-yl)piperazin-1-yl)(2-fluorophenyl)methanone (**4b**).* Prepared by method A, white solid, mp 145–147 °C, yield 77%. ^{1}H NMR (400 MHz, $CDCl_3$), δ(ppm): 8.22 (1H, d, J = 5.5 Hz), 7.41 (2H, m), 7.22 (2H, m), 7.09 (3H, m), 6.15 (1H, d, J = 5.5 Hz), 3.82 (4H, m), 3.66 (2H, m), 3.34 (2H, m); ^{13}C NMR (100 MHz, $CDCl_3$), δ(ppm): 158.9, 165.4, 161.2, 160.0, 157.9, 153.3, 135.1, 131.5, 129.3, 125.6, 124.8, 123.9, 123.8, 120.9, 115.8, 96.8, 46.7, 44.0, 43.5, 41.8; HRMS (ESI)+ calculated for $C_{21}H_{18}Cl_2FN_4O_2$, $[M+H]+$: m/z 447.0791, found 447.0793; Purity: 98.4% (HPLC).

*4.2.4.3. (3-chlorophenyl)(4-(4-(3,5-dichlorophenoxy)pyrimidin-2-yl)piperazin-1-yl)methanone (**4c**).* Prepared by method A, off-white solid, mp 118–120 °C, yield 88%. ^{1}H NMR (400 MHz, $CDCl_3$), δ(ppm): 8.23 (1H, d, J = 5.6 Hz), 7.41 (2H, m), 7.37 (1H, m), 7.29 (1H, d, J = 7.4 Hz), 7.23 (1H, dd, J = 1.7, 1.7 Hz), 7.09 (2H, d, J = 1.8 Hz), 6.16 (1H, d, J = 5.5 Hz), 3.66 (8H, m); ^{13}C NMR (100 MHz, $CDCl_3$), δ(ppm): 169.0, 168.9, 161.2, 160.0, 153.3, 137.2, 135.1, 134.7, 130.1, 130.0, 127.3, 125.6, 125.2, 120.9, 120.9, 96.9, 47.4, 43.0, 43.9, 42.0; HRMS (ESI)+ calculated for $C_{21}H_{18}Cl_3N_4O_2$, $[M+H]+$: m/z 463.0495, found 463.0492; Purity: 98.8% (HPLC).

*4.2.4.4. (4-(4-(3,5-dichlorophenoxy)pyrimidin-2-yl)piperazin-1-yl)(2,4-dichlorophenyl)methanone (**4d**).* Prepared by method A, off-white solid, mp 155–157 °C, yield 86%. ^{1}H NMR (400 MHz, $CDCl_3$), δ(ppm): 8.23 (1H, d, J = 5.5 Hz), 7.44 (1H, d, J = 1.9 Hz), 7.33 (1H, m), 7.23 (2H, m), 7.08 (2H, d, J = 1.9 Hz), 6.16 (1H, d, J = 5.5 Hz), 3.81 (4H,

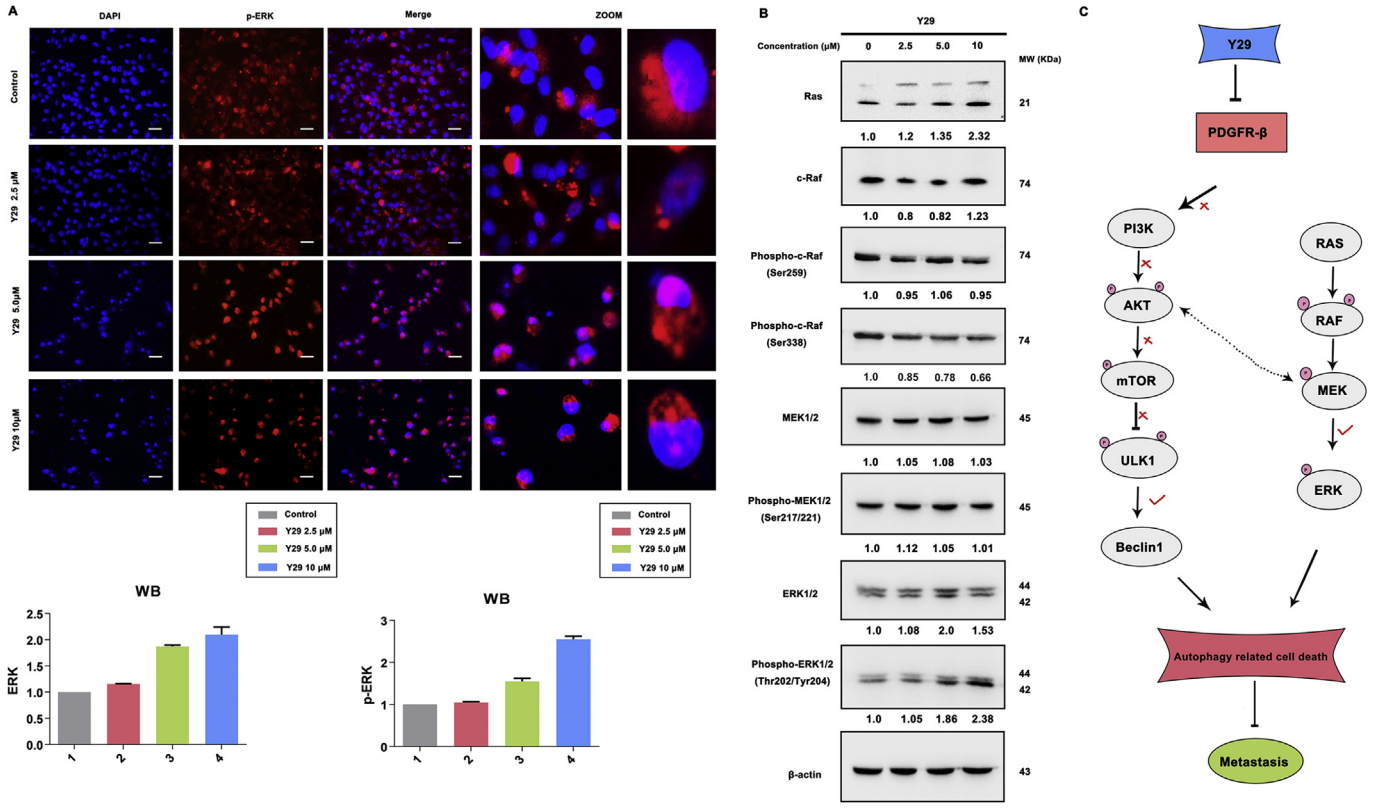

Fig. 6. Y29 could enhance MDA-MB-231 cells autophagy-related cell death through AKT-MAPK feedback loop. (A) Y29 could obviously up-regulate the expression of *p*-ERK. The expression of *p*-ERK (Thr202/Tyr204) was detected by immunocytochemistry. Red: TRITC-*anti-p*-ERK; blue: DAPI. Scale bar: 50 μM. (B) MDA-MB-231 cells were treated with different concentrations of Y29 for 24 h and then the expressions of RAS-ERK signaling were detected by western blot analysis. β-actin was measured as loading control. (C) The schematic model of Y29-induced metastasis inhibition through autophagy-related cell death pathways. (For interpretation of the references to colour in this figure legend, the reader is referred to the web version of this article.)

m), 3.65 (2H, m), 3.25 (2H, m); ^{13}C NMR (100 MHz, $CDCl_3$), δ(ppm): 168.9, 166.2, 161.2, 160.0, 153.5, 135.8, 135.1, 134.0, 131.3, 129.7, 128.8, 127.8, 125.6, 120.9, 120.9, 96.9, 46.4, 43.9, 43.5, 41.6; HRMS (ESI)+ calculated for $C_{21}H_{17}Cl_4N_4O_2$, [M+H]+: *m/z* 497.0106, found 497.0110; Purity: 96.3% (HPLC).

*4.2.4.5. (4-(4-(2,4-dichlorophenoxy)pyrimidin-2-yl)piperazin-1-yl)(4 (trifluoromethyl)phenyl)methanone (**4e**).* Prepared by method A, off-white solid, mp 141–144 °C, yield 71%. ^{1}H NMR (400 MHz, $CDCl_3$), δ(ppm): 8.23 (1H, d, *J* = 5.5 Hz), 7.70 (2H, d, *J* = 8.0 Hz), 7.53 (2H, d, *J* = 8.0 Hz), 7.23 (1H, s), 7.08 (2H, d *J* = 1.8 Hz), 6.17 (1H, d, *J* = 5.5 Hz), 3.82 (4H, s), 3.64 (2H, s), 3.40 (2H, s); ^{13}C NMR (100 MHz, $CDCl_3$), δ(ppm): 169.1, 169.0, 161.2, 160.0, 153.3, 139.0, 135.1, 131.9, 127.5, 127.5, 125.8, 125.5, 125.0, 122.3, 120.9, 120.9, 96.9, 47.3, 44.0, 43.5, 42.0; HRMS (ESI)+ calculated for $C_{22}H_{18}Cl_2F_3N_4O_2$, [M+H]+: *m/z* 497.0759, found 497.0764; Purity: 96.5% (HPLC).

*4.2.4.6. (4-(4-(3,5-dichlorophenoxy)pyrimidin-2-yl)piperazin-1-yl)(3-(trifluoromethyl)phenyl)methanone (**4f**).* Prepared by method A, off-white solid, mp 146–149 °C, yield 75%. ^{1}H NMR (400 MHz, $CDCl_3$), δ(ppm): 8.24 (1H, d, *J* = 5.4 Hz), 7.71 (2H, m), 7.59 (2H, m), 7.23 (1H, m), 7.09 (2H, d, *J* = 1.8 Hz), 6.17 (1H, d, *J* = 5.4 Hz), 3.74 (6H, m), 3.43 (2H, s); ^{13}C NMR (100 MHz, $CDCl_3$), δ(ppm): 169.0, 168.9, 161.2, 160.0, 153.3, 136.3, 135.1, 131.2, 130.4, 129.2, 126.7, 125.6, 124.2, 123.6, 120.9, 120.9, 96.9, 47.3, 43.7, 43.7, 42.2; HRMS (ESI)+ calculated for $C_{22}H_{18}Cl_2F_3N_4O_2$, [M+H]+: *m/z* 497.0759, found 497.0762; Purity: 99.5% (HPLC).

*4.2.4.7. Benzo[d][1,3]dioxol-5-yl(4-(4-(3,5-dichlorophenoxy)pyrimidin-2-yl)piperazin-1-yl)methanone (**4g**).* Prepared by method A, off-white solid, mp 78–81 °C, yield 88%. ^{1}H NMR (400 MHz, $CDCl_3$), δ(ppm): 8.23 (1H, d, *J* = 5.5 Hz), 7.23 (1H, m), 7.09 (2H, d, *J* = 1.8 Hz), 6.93 (2H, m), 6.83 (2H, d, *J* = 7.9 Hz), 6.15 (1H, d, *J* = 5.4 Hz), 6.01 (2H, s), 3.67 (7H, m); ^{13}C NMR (100 MHz, $CDCl_3$), δ(ppm): 170.2, 168.9, 161.3, 160.0, 153.3, 149.0, 147.7, 135.1, 129.0, 125.6, 121.7, 120.9, 120.9, 108.3, 108.1, 101.5, 96.7, 43.8, 43.9, 38.6, 38.6; HRMS (ESI)+ calculated for $C_{22}H_{19}Cl_2N_4O_4$, [M+H]+: *m/z* 473.0783, found 473.0787; Purity: 98.1% (HPLC).

*4.2.4.8. N-(4-(4-(4-(3,5-dichlorophenoxy)pyrimidin-2-yl)piperazine-1-carbonyl)phenyl)acetamide (**4h**).* Prepared by method B, off-white solid, mp 187–189 °C, yield 78%. ^{1}H NMR (400 MHz, $CDCl_3$), δ(ppm): 8.23 (1H, d, *J* = 5.6 Hz), 8.08 (1H, s), 7.50 (2H, d, *J* = 8.4 Hz), 7.33 (2H, d, *J* = 8.4 Hz), 7.23 (1H, m), 7.09 (2H, d, *J* = 1.8 Hz), 6.15 (1H, d, *J* = 5.6 Hz), 3.72 (8H, m), 2.17 (3H, s); ^{13}C NMR (100 MHz, $CDCl_3$), δ(ppm): 170.5, 169.0, 168.9, 161.2, 160.0, 153.3, 139.8, 135.1, 130.6, 128.2, 125.6, 120.9, 120.9, 119.7, 96.8, 43.8, 38.6, 24.5; HRMS (ESI)+ calculated for $C_{23}H_{22}Cl_2N_5O_3$, [M+H]+: *m/z* 486.1100, found 486.1108; Purity: 95.4% (HPLC).

*4.2.4.9. (4-(4-(3,5-dichlorophenoxy)pyrimidin-2-yl)piperazin-1-yl)(3-hydroxyphenyl)methanone (**4i**).* Prepared by method B, off-white solid, mp 194–196 °C, yield 92%. ^{1}H NMR (400 MHz, $CDCl_3$), δ(ppm): 8.22 (1H, d, *J* = 5.5 Hz), 7.21 (2H, m), 7.09 (2H, d, *J* = 1.8 Hz), 6.93 (1H, m), 6.84 (2H, m), 6.16 (1H, d, *J* = 5.5 Hz), 3.79 (4H, s), 3.62 (2H, s), 3.44 (2H, s); ^{13}C NMR (100 MHz, $CDCl_3$), δ(ppm): 171.1, 169.0, 161.2, 160.0, 157.0, 153.3, 140.0, 135.1, 130.0,

126.0, 120.9, 120.9, 118.1, 117.7, 114.6, 96.9, 44.1, 43.5, 42.2, 38.7; HRMS (ESI)+ calculated for $C_{21}H_{19}Cl_2N_4O_3$, [M+H]+: *m/z* 445.0834, found 445.0836; Purity: 97.1% (HPLC).

*4.2.4.10. 2-(3,5-bis(trifluoromethyl)phenyl)-1-(4-(4-(3,5-dichlorophenoxy)pyrimidin-2-yl)piperazin-1-yl)-2-methylpropan-1-one (**4j**).* Prepared by method B, off-white solid, mp 104–107 °C, yield 83%. ^{1}H NMR (400 MHz, $CDCl_3$), δ(ppm): 8.16 (1H, d, *J* = 5.5 Hz), 7.79 (1H, s), 7.70 (2H, s), 7.22 (1H, m), 7.05 (2H, d, *J* = 1.7 Hz), 6.10 (1H, d, *J* = 5.5 Hz), 1.62 (8H, m); ^{13}C NMR (100 MHz, $CDCl_3$), δ(ppm): 173.4, 168.8, 161.1, 160.0, 135.2, 149.1, 135.2, 133.0, 132.6, 132.3, 131.2, 125.6, 125.1, 124.5, 121.8, 120.8, 120.8, 96.8, 47.3, 43.3, 43.2, 42.2, 43.1, 28.3; HRMS (ESI)+ calculated for $C_{26}H_{23}Cl_2F_6N_4O_2$, [M+H]+: *m/z* 607.1102, found 607.1104; Purity: 98.2% (HPLC).

*4.2.4.11. (4-(4-(3,5-dichlorophenoxy)pyrimidin-2-yl)piperazin-1-yl)(5-methylpyrazin-2-yl)methanone (**4k**).* Prepared by method B, off-white solid, mp 128–131 °C, yield 79%. ^{1}H NMR (400 MHz, $CDCl_3$), δ(ppm): 8.88 (1H, d, *J* = 1.2 Hz), 8.42 (1H, s), 8.24 (1H, d, *J* = 5.3 Hz), 7.24 (1H, dd, *J* = 1.8,1.9 Hz), 7.10 (2H, d, *J* = 1.5 Hz), 6.16 (1H, d, *J* = 5.5 Hz), 3.84 (4H, s), 3.71 (4H, d, *J* = 10.8 Hz), 2.63 (3H, s); ^{13}C NMR (100 MHz, $CDCl_3$), δ(ppm): 168.9, 165.7, 161.2, 160.0, 155.1, 153.3, 145.9, 144.9, 142.2, 135.1, 125.6, 120.9, 120.9, 96.7, 46.9, 44.1, 43.5, 42.4; HRMS (ESI)+ calculated for $C_{20}H_{19}Cl_2N_6O_2$, [M+H]+: *m/z* 445.0947, found 445.0958; Purity: 99.3% (HPLC).

*4.2.4.12. (4-chloropyridin-2-yl)(4-(4-(3,5-dichlorophenoxy)pyrimidin-2-yl)piperazin-1-yl)methanone (**4l**).* Prepared by method B, off-white solid, mp 139–141 °C, yield 85%. ^{1}H NMR (400 MHz, $CDCl_3$), δ(ppm): 8.49 (1H, d, *J* = 5.3 Hz), 8.23 (1H, d, *J* = 5.5 Hz), 7.72 (1H, d, *J* = 1.9 Hz), 7.37 (1H, dd, *J* = 5.4, 2.0 Hz), 7.23 (1H, m), 7.10 (2H, d, *J* = 1.8 Hz), 6.15 (1H, d, *J* = 5.5 Hz), 3.83 (4H, s), 3.72 (2H, s), 3.64 (2H, m); ^{13}C NMR (100 MHz, $CDCl_3$), δ(ppm): 168.9, 166.4, 161.2, 160.0, 155.0, 153.3, 149.2, 145.4, 135.1, 125.6, 125.1, 124.8, 120.9, 120.9, 96.7, 46.9, 44.1, 43.5, 42.4; HRMS (ESI)+ calculated for $C_{20}H_{17}Cl_3N_5O_2$, [M+H]+: *m/z* 464.0448, found 464.0456; Purity: 96.2% (HPLC).

*4.2.4.13. (4-(4-(3,5-dichlorophenoxy)pyrimidin-2-yl)piperazin-1-yl)(quinolin-6-yl)methanone (**4m**).* Prepared by method B, off-white solid, mp 78–81 °C, yield 70%. ^{1}H NMR (400 MHz, $CDCl_3$), δ(ppm): 8.98 (1H, dd, *J* = 4.2, 1.6 Hz), 8.24 (1H, d, *J* = 5.5 Hz), 8.21 (1H, d, *J* = 8.0 Hz), 8.17 (1H, d, *J* = 8.7 Hz), 7.93 (1H, d, *J* = 1.5 Hz), 7.74 (1H, dd, *J* = 8.4, 1.6 Hz), 7.48 (1H, dd, *J* = 8.3, 4.2 Hz), 7.21 (1H, m), 7.09 (2H, d, *J* = 1.6 Hz), 6.17 (1H, d, *J* = 5.5 Hz), 3.84 (4H, m), 3.68 (2H, m), 3.51 (2H, m); ^{13}C NMR (100 MHz, $CDCl_3$), δ(ppm): 170.0, 168.9, 161.2, 160.0, 153.3, 151.7, 148.5, 136.5, 135.1, 133.6, 130.1, 127.8, 127.1, 125.6, 122.0, 120.9, 120.9, 96.9, 43.7, 31.4, 30.2, 29.7; HRMS (ESI)+ calculated for $C_{24}H_{20}Cl_2N_5O_2$, [M+H]+: *m/z* 480.0994, found 480.0997; Purity: 99.0% (HPLC).

*4.2.4.14. 5-(4-(4-(3,5-dichlorophenoxy)pyrimidin-2-yl)piperazine-1-carbonyl)pyrrolidin-2-one (**4n**).* Prepared by method B, colorless oil, yield 84%. ^{1}H NMR (400 MHz, $CDCl_3$), δ(ppm): 8.24 (1H, d, *J* = 5.4 Hz), 7.25 (1H, m), 7.10 (2H, d, *J* = 1.8 Hz), 6.56 (1H, s), 6.18 (1H, d, *J* = 5.5 Hz), 4.52 (1H, dd, *J* = 7.8, 5.2 Hz), 3.69 (6H, m), 3.47 (2H, m); ^{13}C NMR (100 MHz, $CDCl_3$), δ(ppm): 178.1, 170.0, 169.0, 161.1, 160.0, 153.3, 135.1, 125.7, 120.9, 120.9, 97.0, 54.1, 44.6, 43.7, 43.4, 42.0, 39.4, 25.4; HRMS (ESI)+ calculated for $C_{19}H_{20}Cl_2N_5O_3$, [M+H]+: *m/z* 436.0943, found 436.0948; Purity: 98.2% (HPLC).

*4.2.4.15. (4-(4-(3, 5-dichlorophenoxy) pyrimidin-2-yl) piperazin-1-yl)(indolin-2-yl) methanone (**4o**).* Prepared by method B, white solid, mp 160–163 °C, yield 71%. ^{1}H NMR (400 MHz, $CDCl_3$), δ(ppm): 8.24 (1H, d, *J* = 5.5 Hz),7.26 (1H, m), 7.10 (2H, d, *J* = 1.69 Hz), 7.04 (2H, d, *J* = 7.5 Hz), 6.78 (1H, d, *J* = 7.5 Hz), 6.74 (1H, t, *J* = 15.1 Hz),6.17 (1H, d, *J* = 5.5 Hz), 4.57 (1H, dd, *J* = 10.7, 5.5 Hz), 3.59 (10H, m), 3.15 (1H, dd, *J* = 15.7, 5.5 Hz); ^{13}C NMR (100 MHz, $CDCl_3$), δ(ppm): 172.5, 169.0, 161.2, 160.0, 153.3, 151.0, 135.1, 127.9, 126.8, 125.7, 124.3, 120.9, 119.8, 111.3, 96.9, 58.2, 44.7, 43.6, 43.5, 42.1; HRMS (ESI)+ calculated for $C_{23}H_{22}Cl_2N_5O_2$, [M+H]+: *m/z* 470.1151, found 470.1154; Purity: 95.4% (HPLC).

*4.2.4.16. (4-(4-(3,5-dichlorophenoxy)pyrimidin-2-yl)piperazin-1-yl)(1H-pyrrol-2-yl)methanone (**4p**).* Prepared by method B, off-white solid, mp 198–200 °C, yield 73%. ^{1}H NMR (400 MHz, $CDCl_3$), δ(ppm): 9.78 (1H, s), 8.24 (1H, d, *J* = 5.5 Hz), 7.11 (2H, d, *J* = 1.8 Hz), 6.93 (1H, m), 6.54 (1H, m), 6.26 (1H, dd, *J* = 6.3, 2.7 Hz), 6.15 (1H, d, *J* = 5.5 Hz),3.83 (10H, m); ^{13}C NMR (100 MHz, $CDCl_3$), δ(ppm): 169.0, 162.0, 161.2, 160.0, 153.3, 135.1, 125.6, 124.4, 121.3, 120.9, 120.9, 112.3, 110.0, 96.6, 43.6, 43.6, 43.6, 43.6; HRMS (ESI)+ calculated for $C_{19}H_{18}Cl_2N_5O_2$, [M+H]+: *m/z* 418.0838, found 418.0842; Purity: 98.7% (HPLC).

*4.2.5. Synthesis of compounds **5a-g***

*4.2.5.1. 4-(2,4-dichlorophenoxy)-2-(4-(phenylsulfonyl)piperazin-1-yl)pyrimidine (**5a**).* Prepared by method A, white solid, mp 147–149 °C, yield 84%. ^{1}H NMR (400 MHz, $CDCl_3$), δ(ppm): 8.17 (1H, d, *J* = 5.5 Hz), 7.75 (2H, m), 7.60 (1H, m), 7.53 (2H, m), 7.24 (1H, s), 7.05 (2H, d, *J* = 1.8 Hz), 6.09 (1H, d, *J* = 5.5 Hz), 3.79 (4H, s), 3.02 (4H, dd, *J* = 5.1, 5.0 Hz); ^{13}C NMR (100 MHz, $CDCl_3$), δ(ppm): 168.9, 160.9, 160.0, 153.2, 135.5, 135.1, 133.0, 129.2, 129.2, 127.8, 127.8, 125.6, 120.9, 120.9, 96.8, 45.8, 45.8, 43.1, 43.1; HRMS (ESI)+ calculated for $C_{20}H_{19}Cl_2N_4O_3S$, [M+H]+: *m/z* 465.0555, found 465.0557; Purity: 99.2% (HPLC).

*4.2.5.2. 2-(4-((4-(tert-butyl)phenyl)sulfonyl)piperazin-1-yl)-4-(2,4-dichlorophenoxy)pyrimidine (**5b**).* Prepared by method A, white solid, mp 151–153 °C, yield 79%. ^{1}H NMR (400 MHz, $CDCl_3$), δ(ppm): 8.17 (1H, d, *J* = 5.5 Hz), 7.66 (2H, d, *J* = 8.6 Hz), 7.52 (2H, d, *J* = 8.6 Hz), 7.24 (1H, s), 7.05 (2H, d, *J* = 1.8 Hz), 6.09 (1H, d, *J* = 5.5 Hz), 3.79 (4H, s), 3.03 (4H, dd, *J* = 5.1, 5.0 Hz), 1.33 (9H, s); ^{13}C NMR (100 MHz, $CDCl_3$), δ(ppm): 168.9, 161.0, 160.0, 156.8, 153.2, 135.1, 132.4, 127.7, 127.7, 126.1, 126.1, 125.6, 120.9, 120.9, 96.7, 45.8, 45.8, 43.0, 43.0, 35.2, 31.1, 31.1, 31.1; HRMS (ESI)+ calculated for $C_{24}H_{27}Cl_2N_4O_3S$, [M+H]+: *m/z* 521.1181, found 521.1184; Purity: 96.9% (HPLC).

*4.2.5.3. 4-(2,4-dichlorophenoxy)-2-(4-((2-methoxyphenyl)sulfonyl) piperazin-1-yl)pyrimidine (**5c**).* Prepared by method A, white solid, mp 123–126 °C, yield 82%. ^{1}H NMR (400 MHz, $CDCl_3$), δ(ppm): 8.19 (1H, d, *J* = 5.5 Hz), 7.87 (1H, dd, *J* = 7.8, 1.6 Hz), 7.51 (1H, m), 7.23 (1H, dd, *J* = 1.8, 1.7 Hz), 7.07 (2H, d, *J* = 1.8 Hz), 7.01 (2H, m), 6.10 (1H, d, *J* = 5.5 Hz), 3.90 (3H s), 3.76 (4H, m), 3.25 (4H, dd, *J* = 5.1, 5.0 Hz); ^{13}C NMR (100 MHz, $CDCl_3$), δ(ppm): 168.9, 161.1, 156.9, 156.9, 153.3, 135.1, 124.7, 131.8, 126.1, 125.6, 120.8, 120.8, 120.5, 112.3, 96.6, 56.0, 45.7, 45.7, 43.8, 43.8; HRMS (ESI)+ calculated for $C_{21}H_{21}Cl_2N_4O_4S$, [M+H]+: *m/z* 495.0661, found 495.0663; Purity: 98.5% (HPLC).

*4.2.5.4. 4-(3,5-dichlorophenoxy)-2-(4-((4-methoxyphenyl)sulfonyl) piperazin-1-yl)pyrimidine (**5d**).* Prepared by method A, white solid, mp 126–128 °C, yield 89%. ^{1}H NMR (400 MHz, $CDCl_3$), δ(ppm): 8.16 (1H, d, *J* = 5.5 Hz), 7.68 (2H, m), 7.24 (1H, s), 7.05 (2H, d, *J* = 1.8 Hz), 6.99 (1H, m), 6.97 (1H, m), 6.09 (1H, d, *J* = 5.5 Hz), 3.87 (3H, s), 3.78 (4H, m), 2.99 (4H, m); ^{13}C NMR (100 MHz, $CDCl_3$), δ(ppm): 168.9, 163.2, 160.9, 160.0, 153.3, 135.1, 130.0, 130.0, 127.0, 125.6, 120.9, 120.9, 114.3, 114.3, 96.7, 55.6, 45.8, 45.8, 43.0, 43.0; HRMS (ESI)+ calculated for $C_{21}H_{21}Cl_2N_4O_4S$, [M+H]+: *m/z* 495.0661, found 495.0665; Purity: 98.3% (HPLC).

*4.2.5.5. 4-(3,5-dichlorophenoxy)-2-(4-(pyridin-3-ylsulfonyl)piperazin-1-yl)pyrimidine (**5e**).* Prepared by method A, white solid, mp 176–179 °C, yield 79%. ^{1}H NMR (400 MHz, $CDCl_3$), δ(ppm): 8.98 (1H, m), 8.82 (1H, dd, J = 4.9, 1.6 Hz), 8.17 (1H, d, J = 5.5 Hz), 8.04 (1H, m), 7.48 (1H, m), 7.24 (1H, dd, J = 1.8, 1.7 Hz), 7.05 (2H, d, J = 1.8 Hz), 6.12 (1H, d, J = 5.5 Hz), 3.81 (4H, m), 3.07 (4H, dd, J = 5.1, 5.0 Hz); ^{13}C NMR (100 MHz, $CDCl_3$), δ(ppm): 168.9, 160.9, 160.0, 153.6, 153.2, 148.5, 135.4, 135.1, 131.5, 125.7, 123.8, 120.9, 120.9, 97.0, 45.6, 45.6, 43.0, 43.0; HRMS (ESI)+ calculated for $C_{19}H_{18}Cl_2N_5O_3S$, [M+H]+: m/z 466.0507, found 466.0508; Purity: 99.9% (HPLC).

*4.2.5.6. 4-(2, 4-dichlorophenoxy)-2-(4-((4-fluorophenyl)sulfonyl) piperazin-1-yl)pyrimidine (**5f**).* Prepared by method A, white solid, mp 164–166 °C, yield 77%. ^{1}H NMR (400 MHz, $CDCl_3$), δ(ppm): 8.17 (1H, d, J = 5.5 Hz), 7.76 (2H, m), 7.31 (3H, m), 7.05 (2H, d, J = 1.8 Hz), 6.11 (1H, d, J = 5.5 Hz), 3.82 (4H, s), 3.01 (4H, dd, J = 5.1, 5.0 Hz); ^{13}C NMR (100 MHz, $CDCl_3$), δ(ppm): 168.9, 166.6, 165.4, 160.9, 159.9, 153.2, 135.1, 131.6, 130.5, 130.4, 125.6, 120.9, 120.9, 116.4, 116.3, 96.9, 45.7, 45.7, 43.0, 43.9; HRMS (ESI)+ calculated for $C_{20}H_{18}Cl_2FN_4O_3S$, [M+H]+: m/z 483.0461, found 483.0466; Purity: 98.3% (HPLC).

*4.2.5.7. 4-((4-(4-(2, 4-dichlorophenoxy) pyrimidin-2-yl) piperazin-1-yl) sulfonyl) benzonitrile (**5g**).* Prepared by method A, white solid, mp 221–224 °C, yield 72%. ^{1}H NMR (400 MHz, $CDCl_3$), δ(ppm): 8.17 (1H, d, J = 5.5 Hz), 7.87 (2H, d, J = 8.6 Hz), 7.83 (2H, d, J = 8.6 Hz), 7.24(1H, m), 7.05 (2H, d, J = 1.8 Hz), 6.13 (1H, d, J = 5.5 Hz), 3.80 (4H, s), 3.05 (4H, dd, J = 5.1, 5.0 Hz); ^{13}C NMR (100 MHz, $CDCl_3$), δ(ppm): 168.9, 160.8, 160.0, 153.2, 140.1, 135.1, 133.0, 133.0, 128.3, 128.3, 125.6, 120.9, 120.9, 117.1, 116.8, 97.0, 45.7, 45.7, 43.0, 43.0; HRMS (ESI)+ calculated for $C_{21}H_{18}Cl_2N_5O_3S$, [M+H]+: m/z 490.0507, found 490.0510; Purity: 97.9% (HPLC).

*4.2.6. Synthesis of compounds **6a-g***

To a solution of intermediate **3** (1 mmol) and DIEA (1.1 mmol) in dichloromethane (10 ml), a solution of R_3NCO (1.1 eq) in dichloromethane (2 ml) was added dropwise at 0 °C for 6 h. Upon completion removing the solvent under reduced pressure, the crude product was purified by flash chromatography on silica gel, eluting with dichloromethane/methanol (5%), yield 80–95%.

*4.2.6.1. 4-(4-(3, 5-dichlorophenoxy) pyrimidin-2-yl)-N-(p-tolyl) piperazine-1-carboxamide (**6a**).* White solid, mp 166–169 °C, yield 76%. ^{1}H NMR (400 MHz, $CDCl_3$), δ(ppm): 8.23 (1H, d, J = 5.5 Hz), 7.23 (2H, m), 7.11 (2H, d, J = 1.8, Hz), 7.08 (2H, m), 6.37 (1H, s), 6.14 (1H, d, J = 5.5 Hz), 3.75 (4H, m), 3.52 (4H, m), 2.29 (3H, s); ^{13}C NMR (100 MHz, $CDCl_3$), δ(ppm): 168.9, 161.2, 160.0, 155.3, 153.4, 136.1, 135.1, 133.0, 129.4, 129.4, 125.6, 120.9, 120.9, 120.4, 120.4, 96.6, 43.6, 43.6, 43.4, 43.4, 20.8; HRMS (ESI)+ calculated for $C_{22}H_{22}Cl_2N_5O_2$, $[M+H]^+$: m/z 458.1151, found 458.1153; Purity: 99.3% (HPLC).

*4.2.6.2. N-(3-chlorophenyl)-4-(4-((2, 4-dichlorophenyl) (oxo)-l4-oxidanyl) pyrimidin-2-yl) piperazine-1-carboxamide (**6b**).* White solid, mp 232–235 °C, yield 80%. ^{1}H NMR (400 MHz, $CDCl_3$), δ(ppm): 8.24 (1H, d, J = 5.5 Hz), 7.45(1H, m), 7.25 (1H, m), 7.19 (2H, m), 7.11 (2H, d, J = 1.8 Hz), 7.00 (1H, m), 6.50 (1H, s), 6.15 (1H, d, J = 5.5 Hz), 3.76 (4H, m), 3.53 (4H, m); ^{13}C NMR (100 MHz, $CDCl_3$), δ(ppm): 168.9, 161.2, 160.0, 154.7, 153.3, 140.1, 135.1, 134.5, 129.8, 125.6, 123.3, 120.9, 120.9, 120.1, 118.1, 96.7, 43.6, 43.6, 43.3, 43.3; HRMS (ESI)+ calculated for $C_{21}H_{19}Cl_3N_5O_2$, $[M+H]^+$: m/z 478.0604, found 478.0607; Purity: 98.9% (HPLC).

4.2.6.3. N-(2-chlorophenyl)-4-(4-(3, 5-dichlorophenoxy)pyrimidin-2-yl)piperazine-1-carboxamide (6c). White solid, mp 114–117 °C, yield 82%. ^{1}H NMR (400 MHz, $CDCl_3$), δ(ppm): 8.24 (1H, d, J = 5.4 Hz), 8.18 (1H, dd, J = 8.4, 1.4 Hz), 7.34 (1H, dd, J = 8.1, 1.4 Hz), 7.25 (2H, m), 7.11 (2H, d, J = 1.8 Hz), 7.01 (1H, s), 6.97 (1H, m), 6.16 (1H, d, J = 5.5 Hz), 3.78 (4H, m), 3.59 (4H, m); ^{13}C NMR (100 MHz, $CDCl_3$), δ(ppm): 168.9, 161.2, 160.0, 154.2, 153.3, 135.6, 135.1, 128.8, 127.8, 125.6, 123.3, 122.4, 121.0, 120.9, 120.9, 96.7, 43.5, 43.5, 43.3, 43.3; HRMS (ESI)+ calculated for $C_{21}H_{19}Cl_3N_5O_2$, $[M+H]^+$: m/z 478.0604, found 478.0606; Purity: 97.0% (HPLC).

*4.2.6.4. 4-(4-(3, 5-dichlorophenoxy) pyrimidin-2-yl)-N-(naphthalen-2-yl) piperazine-1-carboxamide (**6d**).* White solid, mp 192–195 °C, yield 89%. ^{1}H NMR (400 MHz, $CDCl_3$), δ(ppm): 8.24 (1H, d, J = 5.5 Hz), 7.84 (2H, m), 7.66 (1H, d, J = 8.2 Hz), 7.61 (1H, d, J = 7.3 Hz), 7.48 (2H, m), 7.42 (1H, m), 7.24 (1H, dd, J = 1.8, 1.7 Hz), 7.12 (2H, d, J = 1.8 Hz), 6.68 (1H, s), 6.16 (1H, d, J = 5.5 Hz), 3.76 (4H, m), 3.56 (4H, m); ^{13}C NMR (100 MHz, $CDCl_3$), δ(ppm): 168.9, 161.3, 160.0, 156.1, 153.4, 135.1, 134.2, 133.7, 128.7, 128.2, 126.2, 126.0, 125.7, 125.6, 125.4, 121.2, 121.2, 120.9, 120.9, 96.6, 43.8, 43.8, 43.4, 43.4; HRMS (ESI)+ calculated for $C_{25}H_{22}Cl_2N_5O_2$, $[M+H]^+$: m/z 494.1151, found 494.1154; Purity: 95.1% (HPLC).

*4.2.6.5. 4-(4-(2, 4-dichlorophenoxy) pyrimidin-2-yl)-N-(4-(trifluoromethyl) phenyl) piperazine-1-carboxamide (**6e**).* White solid, mp 156–159 °C, yield 78%. ^{1}H NMR (400 MHz, $CDCl_3$), δ(ppm): 8.24 (1H, d, J = 5.5 Hz), 7.53 (2H, d, J = 8.7 Hz), 7.47 (2H, d, J = 8.7 Hz), 7.25 (1H, s), 7.11 (2H, d, J = 1.8 Hz), 6.60 (1H, s), 6.16 (1H, d, J = 5.5 Hz), 3.78 (4H, s), 3.56 (4H, m); ^{13}C NMR (100 MHz, $CDCl_3$), δ(ppm): 168.9, 161.2, 160.0, 154.4, 153.3, 142.1, 135.1, 126.2, 126.1, 125.6, 125.1, 124.7, 120.9, 120.9, 119.2, 119.2, 96.8. 43.7, 43.7, 43.3, 43.3; HRMS (ESI) + calculated for $C_{22}H_{19}Cl_2F_3N_5O_2$, $[M+H]^+$: m/z 512.0868, found 512.0870; Purity: 98.3% (HPLC).

*4.2.6.6. 4-(4-(2, 4-dichlorophenoxy) pyrimidin-2-yl)-N-(4-methoxyphenyl) piperazine-1-carboxamide (**6f**).* White solid, mp 59–62 °C, yield 87%. ^{1}H NMR (400 MHz, $CDCl_3$), δ(ppm): 8.19 (1H, d, J = 5.5 Hz), 7.89 (1H, m), 7.51 (1H, m), 7.23 (1H, m), 7.07 (2H, d, J = 1.8 Hz), 7.02 (2H, m), 6.10 (1H, d, J = 5.5 Hz, 3.90 (3H, s), 3.76 (4H, m), 3.25 (4H, m); ^{13}C NMR (100 MHz, $CDCl_3$), δ(ppm): 168.9, 161.2, 160.0, 156.1, 155.6, 153.4, 135.1, 131.7, 125.6, 122.6, 122.6, 120.9, 120.9, 114.1, 114.1, 96.6, 55.5, 43.6, 43.6, 43.4, 43.4; HRMS (ESI)+ calculated for $C_{22}H_{22}Cl_2N_5O_3$, $[M+H]^+$: m/z 474.1100, found 474.1106; Purity: 97.4% (HPLC).

*4.2.6.7. N-(3, 5-bis (trifluoromethyl) phenyl)-4-(4-(2, 4-dichlorophenoxy) pyrimidin-2-yl) piperazine-1-carboxamide (**6g**).* White solid, mp 138–141 °C, yield 88%. ^{1}H NMR (400 MHz, $CDCl_3$), δ(ppm): 8.25 (1H, d, J = 5.5 Hz), 7.74 (2H, s), 7.64 (1H, s), 7.29 (1H, s), 7.25 (1H, m), 7.10 (2H, d, J = 1.8 Hz), 6.20 (1H, d, J = 5.5 Hz), 3.99 (4H, m), 3.85 (4H, m); ^{13}C NMR (100 MHz, $CDCl_3$), δ(ppm): 182.3, 169.0, 161.0, 160.0, 153.3, 141.1, 135.1, 135.1, 132.2, 125.7, 125.7, 124.3, 123.6, 121.7, 121.0, 121.0, 118.4, 97.1, 48.3, 48.3, 42.7, 42.7; HRMS (ESI)+ calculated for $C_{23}H_{18}Cl_2F_6N_5O_2$, $[M+H]^+$: m/z 580.0742, found 580.0746; Purity: 95.9% (HPLC).

*4.2.7. Synthesis of intermediate **7***

To a solution of intermediate **3** (1 mmol) and DIEA (1.1 mmol) in dichloromethane (10 ml), a solution of bromoacetyl chloride (1.1 eq) in dichloromethane (2 ml) was added dropwise at 0 °C for 4 h. Upon completion removing the solvent under reduced pressure, the crude product was purified by flash chromatography on silica gel, eluting with dichloromethane/methanol (2%), as an off-white solid, yield 90%. 2-bromo-1-(4-(4-(3,5-dichlorophenoxy)pyrimidin-2-yl)piperazin-1-yl)ethan-1-one (**7**) ^{1}H NMR (400 MHz, $CDCl_3$), δ(ppm):8.23 (1H, d, J = 5.5 Hz), 7.25 (2H, m), 7.10 (2H, d, J = 1.8 Hz), 4.10 (2H, s), 3.75 (4H, m), 3.65 (2H, m), 3.54 (2H, m); ^{13}C NMR (100 MHz, DMSO-d_6), δ(ppm): 173.7, 170.1, 166.0, 165.7, 158.5, 139.5, 139.5, 130.5, 126.4, 126.4, 101.7, 49.9, 48.6, 48.1, 47.2, 46.5.

*4.2.8. Synthesis of compounds **8a-b***

To a solution of intermediate **7** (1 mmol) and DIEA (1.5 mmol) in acetonitrile (15 ml), 1-methylpiperazine or morpholine was added dropwise at 0 °C. The resulting mixture was heated to reflux for 6 h. Upon completion the solvent was evaporated under reduced pressure, the crude product was purified by flash chromatography on silica gel, eluting with dichloromethane/methanol (2–4%), as an off-white solid.

*4.2.8.1. 1-(4-(4-(3, 5-dichlorophenoxy) pyrimidin-2-yl) piperazin-1-yl)-2-(4-methylpiperazin-1-yl) ethan-1-one (**8a**).* White solid, mp 120–123 °C, yield 68%. ^{1}H NMR (400 MHz, $CDCl_3$), δ(ppm): 8.23 (1H, d, J = 5.5 Hz), 7.25 (1H, m), 7.11 (2H, d, J = 1.8 Hz), 6.15 (1H, d, J = 5.4 Hz), 3.65 (8H, m), 3.23 (2H, s), 2.63 (8H, m), 2.37 (3H, s); ^{13}C NMR (100 MHz, $CDCl_3$), δ(ppm): 168.9, 168.0, 161.3, 160.0, 153.3, 135.1, 125.6, 120.9, 120.9, 96.7, 60.9, 54.8, 54.8, 52.5, 52.5, 45.5, 45.2, 44.1, 43.6, 42.6; HRMS (ESI)+ calculated for $C_{21}H_{27}Cl_2N_6O_2$, $[M+H]^+$: m/z 465.1573, found 465.1575; Purity: 97.8% (HPLC).

*4.2.8.2. 1-(4-(4-(3, 5-dichlorophenoxy) pyrimidin-2-yl) piperazin-1-yl)-2-(3-methylmorpholino) ethan-1-one (**8b**).* White solid, mp 155–158 °C, yield 72%. ^{1}H NMR (400 MHz, $CDCl_3$), δ(ppm): 8.23 (1H, d, J = 5.5 Hz), 7.25 (1H, m), 7.11 (2H, d, J = 1.8 Hz), 6.15 (1H, d, J = 5.5 Hz), 3.67 (12H, m), 3.21 (2H, s); ^{13}C NMR (100 MHz, $CDCl_3$), δ(ppm): 168.9, 167.9, 161.3, 160.0, 153.3, 135.1, 125.6, 120.9, 120.9, 96.7, 66.9, 66.9, 61.7, 53.5, 53.5, 45.3, 44.1, 43.7, 41.6; HRMS (ESI)+ calculated for $C_{20}H_{24}Cl_2N_5O_3$, $[M+H]^+$: m/z 452.1256, found 452.1256; Purity: 99.2% (HPLC).

*4.2.9. Synthesis of intermediate **9***

To a solution of benzylamine (33 mmol) in ethanol (100 ml), DIEA (66 mmol) and 2, 4-dichloropyrimidine (30 mmol) were added and the resulting mixture was allowed to warm up reflux overnight. Upon completion the solvent was evaporated under reduced pressure. The crude product was purified by flash chromatography on silica gel, eluting with dichloromethane/methanol (3%), as a white solid, yield 76%. *N*-benzyl-2-chloropyrimidin-4-amine (**9**) ^{1}H NMR (400 MHz, $CDCl_3$), δ (ppm): 8.00 (1H, d, J = 5.6 Hz), 7.38–7.30 (5H, m), 6.23 (1H, d, J = 5.9 Hz), 4.55 (2H, s); ^{13}C NMR (100 MHz, DMSO-d_6), δ(ppm): 168.6, 165.1, 160.9, 143.8, 133.7, 133.7, 132.7, 132.3, 132.3, 110.3, 48.6.

*4.2.10. Synthesis of intermediate **10***

To a solution of *intermediate **9*** (10 mmol) in isopropanol (60 ml), DIEA (20 mmol) and *tert*-butyl 1-piperazinecarboxylate (40 mmol) were added at room temperature. The resulting mixture was allowed to warm up reflux for additional overnight. After completion, the residue was evaporated and added 50 ml water, extracted with dichloromethane (3 × 50 ml). The combined organic layers were washed with saturated aqueous sodium bicarbonate and brine, and then dried over anhydrous sodium sulfate. After removing the solvent under reduced pressure to give the crude oil. The crude oil was purified by silica sel flash chromatography (dichloromethane/methanol 50:1) as a white solid, yield 75%.

*4.2.10.1. tert-butyl 4-(4-(benzylamino)pyrimidin-2-yl)piperazine-1-carboxylate (**10**).* ^{1}H NMR (400 MHz, $CDCl_3$), δ(ppm): 8.00 (1H, d, J = 5.8 Hz), 7.36–7.26 (5H, m), 5.71 (1H, d, J = 5.8 Hz), 5.00 (1H, s), 4.52 (1H, d, J = 5.4 Hz), 3.75–3.72 (4H, m), 2.88–2.86 (4H, m), 148 (9H, s); ^{13}C NMR (100 MHz, DMSO-d_6), δ(ppm): 167.5, 166.3, 159.2, 159.0, 145.3, 133.4, 133.4, 132.6, 132.6, 131.9, 131.9, 84.1, 84.1, 49.7, 48.3, 48.3, 48.0, 33.3, 33.3, 33.3.

*4.2.10.2. N-benzyl-2-(piperazin-1-yl) pyrimidin-4-amine (**11**).* ^{1}H NMR (400 MHz, $CDCl_3$), δ(ppm): 8.00 (1H, d, J = 5.8 Hz), 7.36–7.26 (5H, m), 5.71 (1H, d, J = 5.8 Hz), 5.00 (1H, s), 4.52 (1H, d, J = 5.4 Hz), 3.75–3.72 (4H, m), 2.88–2.86 (4H, m), 2.00 (1H, s); ^{13}C NMR (100 MHz, DMSO-d_6), δ(ppm): 167.5, 166.5, 160.2, 145.4, 133.4, 133.4, 132.6, 132.6, 131.8, 131.8, 50.7, 50.7, 49.6, 49.6, 48.5.

*4.2.11. Synthesis of intermediate **12a-c***

4.2.11.1. Prepared by method A

*4.2.11.1.1. 4-(4-(benzylamino) pyrimidin-2-yl)-N-(4-(trifluoromethyl) phenyl) piperazine-1-carboxamide (**12a**).* White solid, mp 183–185 °C, yield 95%. ^{1}H NMR (400 MHz, $CDCl_3$), δ(ppm): 7.89 (1H, d, J = 5.6 Hz), 7.54–748 (4H, m), 7.36–727 (5H, m), 6.66 (1H, s), 5.75 (1H, d, J = 5.7 Hz), 5.03 (1H, brs), 4.53 (2H, d, J = 5.2 Hz), 3.85–3.83 (4H, m), 3.56–3.54 (4H, m); ^{13}C NMR (100 MHz, $CDCl_3$), δ(ppm): 162.7, 161.4, 156.1, 154.5, 142.2, 128.7, 128.7, 127.5, 127.4, 126.2, 125.6, 124.9, 124.6, 122.9, 119.1, 119.1, 45.2, 43.8, 43.8, 43.4, 43.4; HRMS (ESI)+ calculated for $C_{23}H_{24}F_3N_6O$, $[M+H]^+$: m/z 457.1964, found 457.1970; Purity: 98.7% (HPLC).

*4.2.11.1.2. 4-(4-(benzylamino) pyrimidin-2-yl)-N-(2-chlorophenyl) piperazine-1-carboxamide (**12b**).* White solid, mp 131–134 °C, yield 81%. ^{1}H NMR (400 MHz, $CDCl_3$), δ(ppm): 8.20 (1H, dd, J = 8.3, 1.4 Hz), 7.70 (1H, d, J = 5.7 Hz), 7.36–7.23 (7H, m), 7.00 (1H, s), 6.95 (1H, td, J = 7.9, 1.5 Hz), 5.74 (1H, d, J = 5.7 Hz), 5.04 (1H, brs), 4.54 (2H, d, J = 5.3 Hz), 3.88–3.85 (4H, m), 3.60–3.57 (4H, m); ^{13}C NMR (100 MHz, $CDCl_3$), δ(ppm): 162.7, 161.4, 156.2, 154.2, 138.7, 135.7, 128.8, 128.7, 128.7, 127.7, 127.4, 127.4, 123.2, 122.3, 120.9, 45.2, 43.7, 43.7, 43.4, 43.4; HRMS (ESI)+ calculated for $C_{22}H_{24}ClN_6O$, $[M+H]^+$: m/z 423.1700, found 423.1708; Purity: 96.6% (HPLC).

*4.2.11.1.3. (4-(4-(benzylamino) pyrimidin-2-yl) piperazin-1-yl)(2, 4-dichlorophenyl) methanone (**12c**).* White solid, mp 69–72 °C, yield 78%. ^{1}H NMR (400 MHz, $CDCl_3$), δ(ppm): 7.88 (1H, d, J = 5.7 Hz), 7.44 (1H, d, J = 1.9 Hz), 7.35–7.23 (8H, m), 5.74 (1H, d, J = 5.7 Hz), 5.04 (1H, brs), 4.51 (2H, d, J = 5.4 Hz), 3.89–3.82 (4H, m), 3.80–3.66 (2H, m), 3.32–3.17 (2H, m); ^{13}C NMR (100 MHz, $CDCl_3$), δ(ppm): 166.2, 162.7, 161.4, 156.2, 138.6, 135.6, 134.3, 131.3, 129.7, 128.8, 127.7, 127.7, 127.7, 127.4, 46.7, 45.2, 44.0, 43.5, 41.8; HRMS (ESI)+ calculated for $C_{22}H_{22}Cl_2N_5O$, $[M+H]^+$: m/z 442.1201, found 442.1206; Purity: 98.2% (HPLC).

*4.2.12. Synthesis of intermediate **13***

Prepared as intermediate **9**. *2-chloro-N-(3-methoxyphenyl)pyrimidin-4-amine* ^{1}H NMR (400 MHz, $CDCl_3$), δ(ppm): 8.12 (1H, d, J = 5.9 Hz), 7.34 (1H, s), 7.31 (1H, t, J = 8.14 Hz), 6.91–6.87 (2H, m), 6.70 (1H, dd, J = 8.3, 2.0 Hz), 6.63 (1H, d, J = 5.9 Hz), 3.83 (3H, s); ^{13}C NMR (100 MHz, DMSO-d_6), δ(ppm):166.6, 164.9, 164.5, 162.4, 145.1, 135.0, 117.8, 114.0, 111.5, 111.2, 60.2.

*4.2.13. Synthesis of intermediate **14***

Prepared as intermediate 10. tert-butyl 4-(4-((3-methoxyphenyl)amino)pyrimidin-2-yl)piperazine-1-carboxylate ^{1}H NMR (400 MHz, $CDCl_3$), δ(ppm): 8.00 (1H, d, J = 5.7 Hz), 7.24 (1H, t, J = 8.1 Hz), 7.04 (1H, t, J = 2.0 Hz), 6.88 (1H, dd, J = 8.0, 1.1 Hz), 6.66 (1H, dd, J = 8.3, 2.0 Hz), 6.61–6.58 (1H, m), 6.04 (1H, d, J = 5.7 Hz), 3.81 (3H, s), 3.79–3.77 (4H, m), 3.50–3.47 (4H, m), 1.49 (9H, s); ^{13}C NMR (100 MHz, DMSO-d_6), δ(ppm): 166.2, 165.6, 164.8, 161.3, 159.2, 146.6, 134.6, 116.9, 113.0, 110.0, 102.4, 84.2, 84.2, 60.1, 60.1, 48.5, 48.5, 33.3, 33.3, 33.3.

*4.2.14. Synthesis of intermediate **15***

*4.2.14.1. Prepared as intermediate **11**. N-(3-methoxyphenyl)-2-(piperazin-1-yl) pyrimidin-4-amine (15).* ^{1}H NMR (400 MHz, $CDCl_3$), δ(ppm): 8.00 (1H, d, J = 5.7 Hz), 7.24 (1H, t, J = 8.1 Hz), 7.04 (1H, t, J = 2.0 Hz), 6.88 (1H, dd, J = 8.0, 1.1 Hz), 6.66 (1H, dd, J = 8.3, 2.0 Hz), 6.61–6.58 (1H, m), 6.04 (1H, d, J = 5.7 Hz), 3.81 (3H, s), 3.79–3.77 (4H, m), 3.50–3.47 (4H, m); ^{13}C NMR (100 MHz, DMSO-d_6), δ(ppm): 166.4, 165.5, 164.7, 161.3, 146.8, 134.6, 116.8, 112.8, 109.8, 101.9, 60.1,

50.7, 50.7, 50.0, 50.0.

4.2.15. Synthesis of intermediate ***16a-c***

4.2.15.1. Prepared by method A

*4.2.15.1.1. 4-(4-((3-methoxyphenyl) amino) pyrimidin-2-yl)-N-(4-(trifluoromethyl) phenyl) piperazine-1-carboxamide (**16a**).* White solid, mp 183–186 °C, yield 91%. ^{1}H NMR (400 MHz, $CDCl_3$), δ(ppm): 8.01 (1H, d, J = 5.7 Hz), 7.56–7.49 (4H, m), 7.27–7.23 (2H, m), 7.03 (1H, t, J = 1.9 Hz), 6.89 (1H, dd, J = 7.9, 1.2 Hz), 6.68 (1H, dd, J = 8.1, 2.0 Hz), 6.59 (1H, s), 6.54 (1H, s), 6.08 (1H, d, J = 5.7 Hz), 3.92–3.89 (4H, m), 3.82 (3H, s), 3.62–3.59 (4H, m); ^{13}C NMR (100 MHz, DMSO-d_6), δ(ppm): 161.4, 160.8, 160.0, 156.5, 155.0, 144.9, 141.9, 129.9, 126.5, 126.1, 126.1, 123.7, 119.4, 119.4, 112.1, 108.0, 105.3, 97.7, 55.4, 44.0, 44.0, 43.9, 43.9; HRMS (ESI)+ calculated for $C_{23}H_{24}F_3N_6O_2$, $[M+H]^+$: m/z 473.1913, found 473.1916; Purity: 98.1% (HPLC).

*4.2.15.2. N-(2-chlorophenyl)-4-(4-((3-methoxyphenyl) amino) pyrimidin-2-yl) piperazine-1-carboxamide (**16b**).* White solid, mp 123–126 °C, yield 87%. ^{1}H NMR (400 MHz, $CDCl_3$), δ(ppm): 8.20 (1H, dd, J = 8.3, 1.3 Hz), 8.01 (1H, d, J = 5.7 Hz), 7.34 (4H, dd, J = 8.0, 1.3 Hz), 7.27–7.23 (2H, m), 7.03 (2H, s), 6.96 (1H, td, J = 7.9, 1.5 Hz), 6.90 (1H, dd, J = 7.9, 1.4 Hz), 6.67 (1H, dd, J = 8.1, 2.0 Hz), 6.62 (1H, s), 6.07 (1H, d, J = 5.7 Hz), 5.3 (1H, s), 3.93–3.90 (m, 4H), 3.81 (3H, s), 3.65–3.63 (4H, m); ^{13}C NMR (100 MHz, $CDCl_3$), δ(ppm): 161.5, 160.9, 160.3, 157.1, 154.2, 140.0, 135.7, 129.9, 128.8, 127.8, 123.3, 122.4, 121.0, 113.8, 109.3, 107.5, 95.5, 55.3, 43.7, 43.7, 43.4, 43.4; HRMS (ESI)+ calculated for $C_{22}H_{24}ClN_6O_2$, $[M+H]^+$: m/z 439.1649, found 439.1651; Purity: 96.9% (HPLC).

*4.2.15.3. (2, 4-dichlorophenyl)(4-(4-((3-methoxyphenyl) amino) pyrimidin-2-yl) piperazin-1-yl) methanone (**16c**).* White solid, mp 86–89 °C, yield 79%. ^{1}H NMR (400 MHz, $CDCl_3$), δ(ppm): 7.99 (1H, d, J = 5.7 Hz), 7.45 (1H, d, J = 1.7 Hz), 7.33 (1H, dd, J = 8.2, 1.7 Hz), 7.27–7.22 (2H, m), 6.99 (1H, t, J = 1.8 Hz), 6.88 (1H, dd, J = 8.0, 1.2 Hz), 6.66 (1H, dd, J = 8.2, 2.0 Hz), 6.61 (1H, s), 6.10 (1H, d, J = 5.7 Hz), 5.3 (1H, s), 3.93–3.90 (4H, m), 3.81 (3H, s), 3.65–3.63 (4H, m); ^{13}C NMR (100 MHz, $CDCl_3$), δ(ppm): 166.2, 161.5, 160.9, 160.3, 157.1, 139.9, 135.7, 134.2, 131.3, 129.9, 129.7, 128.8, 127.8, 113.8, 109.3, 107.6, 95.6, 55.3, 46.7, 44.1, 43.6, 41.8; HRMS (ESI)+ calculated for $C_{22}H_{22}Cl_2N_5O_2$, $[M+H]^+$: m/z 458.1151, found 458.1155; Purity: 96.6% (HPLC).

4.2.16. Synthesis of intermediate ***17***

To a solution of *m*-anisidine (20 mmol) and 4, 6-dichloropyrimidine (26 mmol) in isopropanol (100 ml), H_2SO_4 (1.5 ml) was added dropwise and the resulting mixture was allowed to warm up reflux overnight. Upon completion the solvent was evaporated under reduced pressure. The crude product was purified by flash chromatography on silica gel, eluting with dichloromethane/methanol (1%), as a white solid, yield 69%. 6-chloro-*N*-(3-methoxyphenyl)pyrimidin-4-amine ^{1}H NMR (400 MHz, $CDCl_3$), δ(ppm): 8.44 (1H, s), 7.74 (1H, s), 7.33 (1H, t, J = 8.1 Hz), 6.89 (2H, s), 6.79 (1H, d, J = 8.1 Hz), 6.75 (1H, s), 3.83 (3H, s); ^{13}C NMR (100 MHz, DMSO-d_6), δ(ppm): 166.5, 164.9, 163.7, 163.2, 145.3, 135.0, 117.9, 113.8, 111.6, 110.3, 60.3.

4.2.17. Synthesis of intermediate ***18***

Prepared as intermediate 10. *tert-butyl 4-(6-((3-methoxyphenyl) amino)pyrimidin-4-yl)piperazine-1-carboxylate* ^{1}H NMR (400 MHz, $CDCl_3$), δ(ppm): 8.26 (1H, s), 7.39 (1H, s), 7.27 (1H, t, J = 8.0 Hz), 6.87–6.86 (2H, m), 6.69 (1H, dd, J = 8.2, 1.5 Hz), 6.61–6.58 (1H, m), 5.96 (1H, s), 3.81 (3H, s), 3.55–3.48 (8H, m), 1.47 (9H, s); ^{13}C NMR (100 MHz, DMSO-d_6), δ(ppm): 167.2, 166.2, 164.9, 162.5, 159.1, 147.1, 134.6, 117.0, 112.0, 110.5, 90.0, 84.3, 84.3, 60.1, 60.1, 48.4, 48.4, 33.3, 33.3, 33.3.

4.2.18. Synthesis of intermediate ***19***

Prepared as intermediate 11. N-(3-methoxyphenyl)-6-(piperazin-1-yl)pyrimidin-4-amine ^{1}H NMR (400 MHz, $CDCl_3$), δ(ppm): 8.26 (1H, s), 7.48 (1H, s), 7.28–7.24 (1H, m), 6.87–6.86 (2H, m), 6.68 (1H, dd, J = 8.2, 1.5 Hz), 5.97 (1H, s), 5.96 (1H, s), 3.81 (3H, s), 3.53–3.50 (4H, m), 2.92–2.90 (4H, m),1.47 (9H, s); ^{13}C NMR (100 MHz, DMSO-d_6), δ(ppm): 167.5, 166.2, 164.8, 162.5, 147.2, 134.6, 117.0, 111.8, 110.5, 89.4, 60.1, 50.4, 50.4, 50.0, 50.0.

4.2.19. Synthesis of intermediate ***20a-c***

4.2.19.1. Prepared by method A

*4.2.19.1.1. 4-(6-((3-methoxyphenyl) amino) pyrimidin-4-yl)-N-(4-(trifluoromethyl) phenyl) piperazine-1-carboxamide (**20a**).* White solid, mp 208–211 °C, yield 97%. ^{1}H NMR (400 MHz, $CDCl_3$), δ(ppm): 8.27 (1H, s), 7.54 (2H, d, J = 8.8 Hz), 7.48 (2H, d, J = 8.8, Hz), 7.28 (1H, t, J = 8.2 Hz), 6.88 (1H, d, J = 1.3 Hz), 6.86 (1H, d, J = 4.5 Hz), 6.70 (1H, dd, J = 8.6, 2.0 Hz), 6.65 (1H, s), 5.95 (1H, s), 3.81 (3H, s), 3.68–3.65 (4H, m), 3.65–3.63 (4H, m); ^{13}C NMR (100 MHz, DMSO-d_6), δ(ppm): 162.5, 161.5, 160.1, 157.8, 154.9, 144.8, 142.4, 129.9, 126.4, 126.1, 123.7, 119.4, 119.4, 112.2, 107.2, 105.8, 84.9, 55.4, 43.7, 43.7, 43.6, 43.6; HRMS (ESI)+ calculated for $C_{23}H_{24}F_3N_6O_2$, $[M+H]^+$: m/z 473.1913, found 473.1913; Purity: 98.4% (HPLC).

*4.2.19.1.2. N-(2-chlorophenyl)-4-(6-((3-methoxyphenyl) amino) pyrimidin-4-yl) piperazine-1-carboxamide (**20b**).* White solid, mp 144–146 °C, yield 88%. ^{1}H NMR (400 MHz, $CDCl_3$), δ(ppm): 8.27 (1H, s), 8.18 (1H, dd, J = 8.3, 14 Hz), 7.33 (2H, d, J = 8.0, 1.3 Hz), 7.30–7.22 (3H, m), 7.00 (1H, s), 6.97 (1H, dd, J = 7.9, 1.5 Hz), 6.88–6.86 (2H, m), 6.70 (1H, dd, J = 8.3, 2.2 Hz), 5.95 (1H, s), 3.81 (3H, s), 3.71–3.69 (4H, m), 3.68–3.66 (4H, m); ^{13}C NMR (100 MHz, $CDCl_3$), δ(ppm): 162.7, 161.4, 160.6, 158.1, 154.1, 140.1, 135.5, 130.2, 128.8, 127.8, 123.4, 122.4, 120.9, 114.6, 109.6, 108.3, 82.3, 55.4, 43.3, 43.3, 43.1, 43.1; HRMS (ESI)+ calculated for $C_{22}H_{24}ClN_6O_2$, $[M+H]^+$: m/z 439.1649, found 439.1654; Purity: 96.5% (HPLC).

*4.2.19.1.3. (2, 4-dichlorophenyl)(4-(6-((3-methoxyphenyl) amino) pyrimidin-4-yl) piperazin-1-yl) methanone (**20c**).* White solid, mp 198–201 °C, yield 78%. ^{1}H NMR (400 MHz, $CDCl_3$), δ(ppm): 8.25 (1H, s), 7.66 (1H, s), 7.44 (1H, d, J = 1.9 Hz), 7.32 (1H, dd, J = 8.2, 1.9 Hz), 7.28–7.23 (2H, m), 6.86–6.84 (2H, m), 6.69 (1H, dd, J = 8.0, 1.5 Hz), 5.96 (1H, s), 3.94–3.76 (m, 2H), 3.80 (3H, s), 3.67–3.51 (4H, m), 3.36–3.27 (2H, m); ^{13}C NMR (100 MHz, $CDCl_3$), δ(ppm): 166.2, 162.8, 161.6, 160.6, 158.0, 140.1, 135.9, 133.9, 131.3, 130.2, 129.7, 128.8, 127.8, 114.6, 109.6, 108.4, 82.5, 55.4, 46.2, 44.2, 43.7, 41.3; HRMS (ESI)+ calculated for $C_{22}H_{22}Cl_2N_5O_2$, $[M+H]^+$: m/z 458.1151, found 458.1152; Purity: 96.6% (HPLC).

4.3. Molecular docking

The discovery Studio 3.5 docking program was adopted here [23]. The preparation of protein structure, including adding hydrogen atoms, removing water molecules, and assigning Charmm forcefield. Goldscore was selected as the score function, and the other parameters were set as default. For each docking study, a total of 10 docking poses were retained. The root-mean square deviation (RMSD) between docking poses were calculated.

4.4. Molecular dynamics (MD) simulations

In the following molecular mechanics (MM) minimizations and MD simulations, the AMBER99 force field and the general AMBER force field (gaff) were used to establish the potential of receptors and ligands, respectively. An appropriate number of sodium counter ions were placed around PDGFR-β-ligand complex to

neutralize the charges of the systems. Finally, the whole system was solvated in a cubic periodic box of TIP3P water molecules, and the distance between the edges of the water box and the closest atom of the solutes was at least 10 Å. To avoid edge effects, periodic boundary conditions were applied during the whole molecular dynamics (MD) simulation. For this system, energy minimization and MD simulation were performed by using the Sander module of the AMBER 12.0. Prior to MD simulations, the entire system was subjected to energy minimization in two stages to remove bad contacts between the complex and the solvent molecules. Firstly, the water molecules and counterions were minimized by freezing the solute using a harmonic constraint of the strength of 100 kcaL mol-1 Å-2. Secondly, the entire system was minimized without restriction. Each stage consisted of a 5000-step steepest descent and a 2000-step conjugate gradient minimization. Finally, 10 ns MD simulations were carried out for each system in an isothermal isobaric ensemble (NPT) under periodic boundary conditions [24].

4.5. Cell culture, antibodies and reagents

MDA-MB-231 were purchased from American Type Culture Collection (ATCC, Manassas, VA, USA). Cells were cultured in DMEM with 10% fetal bovine serum and incubated with 5% CO2.

Antibodies used in this study were as follows: ULK1 (8054, CST, MA, USA), ULK1 (ab128859, Abcam, UK), *p*-ULK1 ser317(12753, CST), *p*-ULK1 ser555 (5869, CST), PDGFR-β (3169, CST), *p*-PDGFR-β Tyr740 (3168, CST), AKT (2920, CST), *p*-AKT Thr308 (13038, CST), *p*-AKT Ser473 (4070, CST), mTOR (2983, CST), *p*-mTOR ser2448 (5536, CST), Beclin-1 (3495, CST), LC3B (3868, CST), p62 (5114, CST), PARP (9532, CST), caspase-3 (9665, CST), Ras (3339,CST), c-Raf (53745, CST), p-*c*-Raf Ser259(9421, CST), p-*c*-Raf Ser338 (9427, CST), MEK (4694, CST), *p*-MEK Ser217/221(9154, CST), ERK (9102, CST), *p*-ERK Thr202/Tyr204 (9101, CST), b-actin (3700, CST). MTT (M2128) was purchased from Sigma- Aldrich (St. Louis, MO, USA).

4.6. Cell viability assay

Cells were dispensed in 96-well plates at a density of 5×10^4 cells/ml. After 24 h incubation, cells were treated with different concentrations of compounds for the indicated time periods. Cell viability was measured by the MTT assay.

4.7. Wound healing assay

Wound healing assays were measured as previous described [25], cells were seeded in 6-well plates, grown until confluent, and wounding was performed with a 10 μL tip that was cut longitudinally. Then MDA-MB-231 cells were cells were treated with different concentrations of compounds for 24 h and observed under a phase contrast microscope.

4.8. Autophagy and apoptosis assays

For the autophagy assay, MDA-MB-231 cells were transfected with GFP/mRFP-LC3 (kindly provided by Prof. Canhua Huang, Sichuan University) then observed under a fluorescence microscope. For apoptosis assay, MDA-MB-231 cells were stained with Annexin V-PI in the dark at 37 °C for 30min, and then measured by FACScan flow cytometry (Becton Dickinson, Franklin Lakes, NJ).

4.9. Immunofluorescence analysis

For immunofluorescence staining, nonspecific antibody binding was blocked by incubating with PBS containing 1.5% goat serum. The MDA-MB-231 cells were sequentially incubated, starting with *p*-ERK antibody (1:200) diluted in PBS containing 1% BSA incubated overnight at 4 °C, followed by addition of fluorescent-labeled secondary antibodies (TRITC, ab6718) for 1 h at room temperature.

4.10. Western blot

Cells were treated with Y29 for indicated times. Both adherent and floating cells were collected. Western blot analysis was carried out. Briefly, the cell pellets were resuspended with lysis buffer consisting of Hepes 50 mM pH 7.4, Triton-X-100 1%, sodium orthovanada 2 mM, sodium fluoride 100 mM, edetic acid 1 mM, PMSF 1 mM, aprotinin (Sigma, MO, USA) 10 mg/L and leupeptin (Sigma) 10 mg/L and lysed at 4 °C for 1 h. After 12,000 rpm centrifugation for 15 min, the protein content of supernatant was determined by the Bio- Rad DC protein assay (Bio-Rad Laboratories, Hercules, CA, USA). Equal amounts of the total protein were separated by 10–15% SDS-PAGE and transferred to PVDF membranes, the membranes were soaked in blocking buffer (5% skimmed milk or BSA). Proteins were detected using primary antibodies, followed by HRP-conjugated secondary antibody and visualized by using ECL as the HRP substrate. Quantification of immunoblot was performed by Quantity One 4.4.

4.11. The enzymatic activity assay

Theses assays were carried out as described previously [26]. All of the enzymatic reactions were conducted at 30 °C for 40 min. The 50 μl reaction mixture contains 40 mM Tris, pH 7.4, 10 mM MgCl2, 0.1 mg/ml BSA, 1 mM DTT, 10 μM ATP, Kinase and the enzyme substrate. The compounds were diluted in 10% DMSO and 5 μl of the dilution was added to a 50 μl reaction so that the final concentration of DMSO is 1% in all of reactions. The assay was performed using Kinase-Glo Plus luminescence kinase assay kit. It measures kinase activity by quantitating the amount of ATP remaining in solution following a kinase reaction. The luminescent signal from the assay is correlated with the amount of ATP present and is inversely correlated with the amount of kinase activity. The IC_{50} values were calculated using nonlinear regression with normalized dose. Response fit using Prism GraphPad sofeware.

4.12. Statistical analysis

All the presented data and results were confirmed by at least three independent experiments. The data are expressed as means ± SEM and analyzed with GraphPad Prism 6.0 software. Statistical comparisons were made by One-way ANOVA and Student's t-test. $P < 0.05$ was considered statistically significant.

Acknowledgements

This work was supported by grants from National Key R&D Program of China (No. 2017YFC0909301) and National Natural Science Foundation of China (Grant No. 81603275 and Grant No. 81602984).

Author contributions

S.-L. Y., Y. Y. and L. O. conceived and designed the experiments; D.-H. Y., Y.-X. Z., L.-J. Z., J. Z. and Y.-Q. Z. performed the experiments; Y.-N. J. and D.-J. S. contributed reagents/materials/analysis tools; D.-H. Y., L.-J. Z. and J. Z. wrote the paper.

Conflicts of interest

The authors declare no conflict of interest.

Appendix A. Supplementary data

Supplementary data related to this article can be found at https://doi.org/10.1016/j.ejmech.2017.08.067.

References

[1] L.A. Torre, F. Bray, R.L. Siegel, J. Ferlay, J. Lortet-Tieulent, A. Jemal, Global cancer statistics, 2012, CA Cancer J. Clin. 65 (2015) 87–108.
[2] L. The, Breast cancer targeted therapy: successes and challenges, Lancet 389 (2017) 2350.
[3] W.J. Irvin Jr., L.A. Carey, What is triple-negative breast cancer? Eur. J. Cancer 44 (2008) 2799–2805.
[4] S. Hurvitz, M. Mead, Triple-negative breast cancer: advancements in characterization and treatment approach, Curr. Opin. Obstet. Gynecol. 28 (2016) 59–69.
[5] M. Kawazu, S. Kojima, T. Ueno, Y. Totoki, H. Nakamura, A. Kunita, W. Qu, J. Yoshimura, M. Soda, T. Yasuda, N. Hama, M. Saito-Adachi, K. Sato, S. Kohsaka, E. Sai, M. Ikemura, S. Yamamoto, T. Ogawa, M. Fukayama, K. Tada, Y. Seto, S. Morishita, S. Hazama, T. Shibata, Y. Yamashita, H. Mano, Integrative analysis of genomic alterations in triple-negative breast cancer in association with homologous recombination deficiency, PLoS Genet. 13 (2017) e1006853.
[6] M.L. Gauthier, H.K. Berman, C. Miller, K. Kozakeiwicz, K. Chew, D. Moore, J. Rabban, Y.Y. Chen, K. Kerlikowske, T.D. Tlsty, Abrogated response to cellular stress identifies DCIS associated with subsequent tumor events and defines basal-like breast tumors, Cancer Cell 12 (2007) 479–491.
[7] C.J. Lord, A. Ashworth, PARP inhibitors: synthetic lethality in the clinic, Science 355 (2017) 1152–1158.
[8] B.J. Monk, D. Lorusso, A. Italiano, S.B. Kaye, M. Aracil, A. Tanovic, M. D'Incalci, Trabectedin as a chemotherapy option for patients with BRCA deficiency, Cancer Treat. Rev. 50 (2016) 175–182.
[9] K.C. Aalders, K. Tryfonidis, E. Senkus, F. Cardoso, Anti-angiogenic treatment in breast cancer: facts, successes, failures and future perspectives, Cancer Treat. Rev. 53 (2017) 98–110.
[10] B. Bao, C. Mitrea, P. Wijesinghe, L. Marchetti, E. Girsch, R.L. Farr, J.L. Boerner, R. Mohammad, G. Dyson, S.R. Terlecky, A. Bollig-Fischer, Treating triple negative breast cancer cells with erlotinib plus a select antioxidant overcomes drug resistance by targeting cancer cell heterogeneity, Sci. Rep. 7 (2017) 44125.
[11] I.S. Babina, N.C. Turner, Advances and challenges in targeting FGFR signalling in cancer, Nat. Rev. Cancer 17 (2017) 318–332.
[12] S.M. Ronnekleiv-Kelly, A. Sharma, N. Ahuja, Epigenetic therapy and chemosensitization in solid malignancy, Cancer Treat. Rev. 55 (2017) 200–208.
[13] X.L. Qian, J. Zhang, P.Z. Li, R.G. Lang, W.D. Li, H. Sun, F.F. Liu, X.J. Guo, F. Gu, L. Fu, Dasatinib inhibits c-src phosphorylation and prevents the proliferation of Triple-Negative Breast Cancer (TNBC) cells which overexpress Syndecan-Binding Protein (SDCBP), PLoS One 12 (2017) e0171169.
[14] T. Bihani, H.K. Patel, H. Arlt, N. Tao, H. Jiang, J.L. Brown, D.M. Purandare, G. Hattersley, F. Garner, Elacestrant (RAD1901), a selective estrogen receptor degrader (SERD), has antitumor activity in multiple ER(+) breast cancer patient-derived xenograft models, Clin. Cancer Res. 23 (2017) 4793–4804.
[15] J. Zhang, P.L. Yang, N.S. Gray, Targeting cancer with small molecule kinase inhibitors, Nat. Rev. Cancer 9 (2009) 28–39.
[16] Jianming Zhang, Priscilla Yang, N. Gray, Targeting cancer with small molecule kinase inhibitors, Nat. Rev. Cancer 9 (1) (2009) 28–39.
[17] D. Gfeller, A. Grosdidier, M. Wirth, A. Daina, O. Michielin, V. Zoete, SwissTargetPrediction: a web server for target prediction of bioactive small molecules, Nucleic Acids Res. 42 (2014) W32–W38.
[18] L.A. Kelley, S. Mezulis, C.M. Yates, M.N. Wass, M.J. Sternberg, The Phyre2 web portal for protein modeling, prediction and analysis, Nat. Protoc. 10 (2015) 845–858.
[19] N. McCarthy, Metastasis: understanding the prowess of mutant p53, Nat. Rev. Cancer 14 (2014) 385.
[20] T.F. Franke, S.I. Yang, T.O. Chan, K. Datta, A. Kazlauskas, D.K. Morrison, D.R. Kaplan, P.N. Tsichlis, The protein kinase encoded by the Akt proto-oncogene is a target of the PDGF-activated phosphatidylinositol 3-kinase, Cell 81 (1995) 727–736.
[21] S. Zimmermann, K. Moelling, Phosphorylation and regulation of Raf by Akt (protein kinase B), Science 286 (1999) 1741–1744.
[22] C. Rommel, B.A. Clarke, S. Zimmermann, L. Nunez, R. Rossman, K. Reid, K. Moelling, G.D. Yancopoulos, D.J. Glass, Differentiation stage-specific inhibition of the Raf-MEK-ERK pathway by Akt, Science 286 (1999) 1738–1741.
[23] G. Wu, D.H. Robertson, C.L. Brooks 3rd, M. Vieth, Detailed analysis of grid-based molecular docking: a case study of CDOCKER-A CHARMm-based MD docking algorithm, J. Comput. Chem. 24 (2003) 1549–1562.
[24] H. Zhong, W. Huang, G. He, C. Peng, F. Wu, L. Ouyang, Molecular dynamics simulation of tryptophan hydroxylase-1: binding modes and free energy analysis to phenylalanine derivative inhibitors, Int. J. Mol. Sci. 14 (2013) 9947–9962.
[25] P. Goulimari, T.M. Kitzing, H. Knieling, D.T. Brandt, S. Offermanns, R. Grosse, Galpha12/13 is essential for directed cell migration and localized Rho-Dia1 function, J. Biol. Chem. 280 (2005) 42242–42251.
[26] M.A. Kashem, R.M. Nelson, J.D. Yingling, S.S. Pullen, A.S. Prokopowicz, J.W. Jones, J.P. Wolak, G.R. Rogers, M.M. Morelock, R.J. Snow, C.A. Homon, S. Jakes, Three mechanistically distinct kinase assays compared: measurement of intrinsic ATPase activity identified the most comprehensive set of ITK inhibitors, J. Biomol. Screen 12 (2007) 70–83.